Examples of the use of XPS in Catalysis Research from the Vohs Group

- Supported monolayer vanadia catalysts
- Ceria/zirconia automotive emissions control catalysts
- Reaction of oxygenates on ZnO
- Pd/ZnO methanol steam reforming catalysts

Introduction

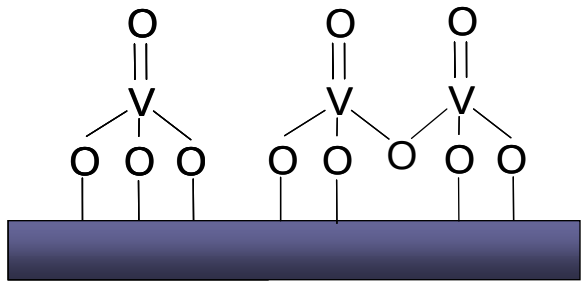

- **Supported monolayer vanadia catalysts are active for:**

$$CH_3OH + O_2 \rightarrow CH_2O + H_2O$$

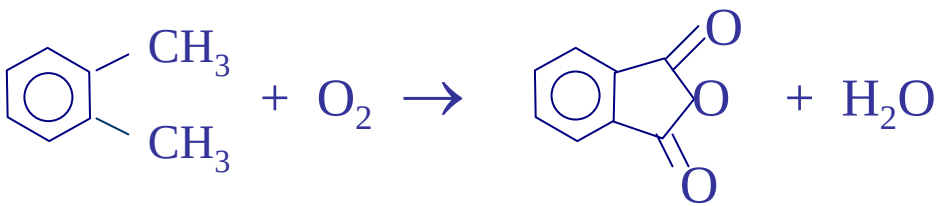

$$NO + NH_3 \rightarrow N_2 + H_2O$$

- **Reactivity depends on:**

  - Identity of the support
    (TiO_2, Al_2O_3, ZrO_2, MgO, CeO_2, etc.)
  - Vanadia coverage

- **Structure-activity relationships not well understood**

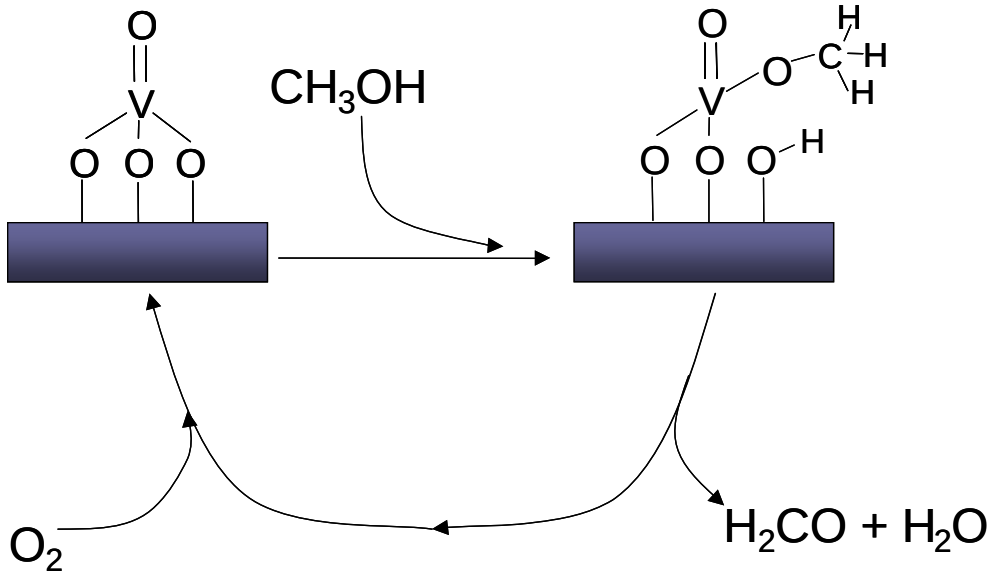

Methanol oxidation activity for vanadia on various oxide supports

Catalyst (monolayer vanadia coverage)	TOF for CH_3OH Oxidation to H_2CO (s^{-1})	Apparent E_a (kJ/mol)
25 % V_2O_5/Al_2O_3	0.068	83.7
7 % V_2O_5/Nb_2O_5	0.4	71.1
6 % V_2O_5/TiO_2	1.1	92.0
4 % V_2O_5/ZrO_2	1.7	75.3
3 % V_2O_5/CeO_2	10.0	83.7

From: Wachs et al., in *Dynamics of Surfaces and Reaction Kinetics in Heterogeneous Catalysis* Elsevier Science B.V., Amsterdam, 1997.

$CH_3OH + O_2 \rightarrow CH_2O + H_2O$ - Mechanism

Hydride Transfer		*Proton/hydrogen Transfer*
$CH_3OH + V* + O* \leftrightarrow V*\text{-}OCH_3 + O*\text{-}H$	(1)	$CH_3OH + V* + O* \leftrightarrow V*\text{-}OCH_3 + O*\text{-}H$
$V*\text{-}OCH_3 \rightarrow CH_2O + V*\text{-}H$	(2 -rds)	$O* + V*\text{-}OCH_3 \rightarrow CH_2O + V* + O*\text{-}H$
$V*\text{-}H + O*\text{-}H \leftrightarrow V* + H_2O + \square$	(3)	$2\ O*\text{-}H \leftrightarrow O* + H_2O + \square$
$O_2 + 2\square \leftrightarrow 2\ O*$	(4)	$O_2 + 2\square \leftrightarrow 2\ O*$

$$\text{TOF} = k_{app} \times \frac{P_{CH_3OH} P_{O_2}^{1/4}}{P_{H_2}^{1/2}}$$

$$k_{app} = (K_1 K_3^{1/2} K_4^{1/4}) \times k_{rds}$$

$$E_{app} \sim E_{rds} + \Delta H_1 + \tfrac{1}{2}\Delta H_3 + \tfrac{1}{4}\Delta H_4$$

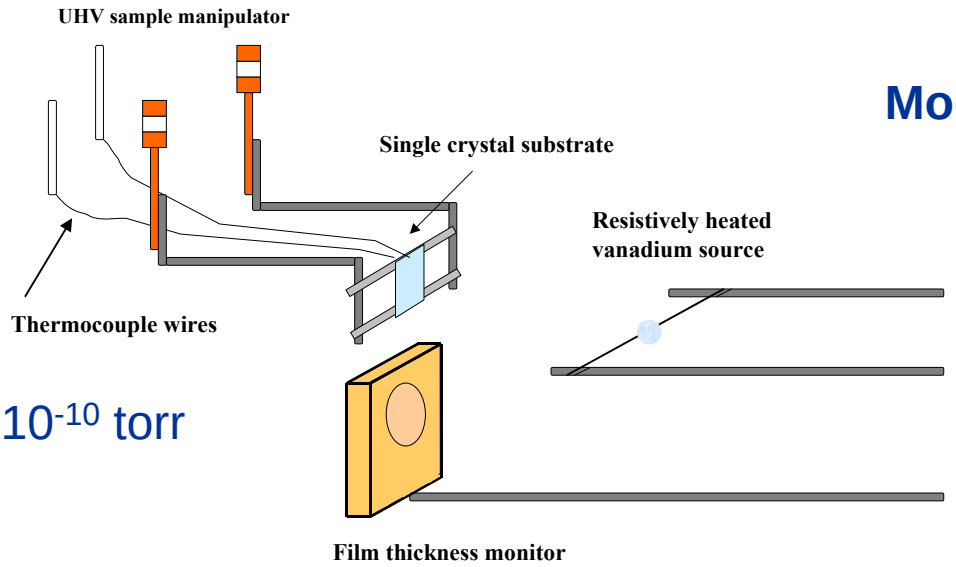

~10^{-10} torr

Model Systems:

Sub-monolayer, monolayer, and multi-layer vanadia films on single crystal metal oxide supports: TiO_2(110), CeO_2 (111), ZrO_2 (100), MgO(100)

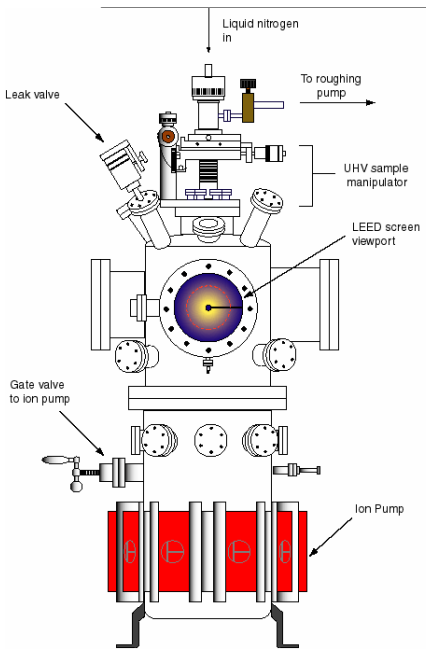

TPD	Temperature Programmed Desorption
AES	Auger Electron Spectroscopy
XPS	X-ray Photoelectron Spectroscopy
LEED	Low Energy Electron Diffraction
HREELS	High Resolution Electron Energy Loss Spectroscopy

Vanadium Deposition on $CeO_2(111)$

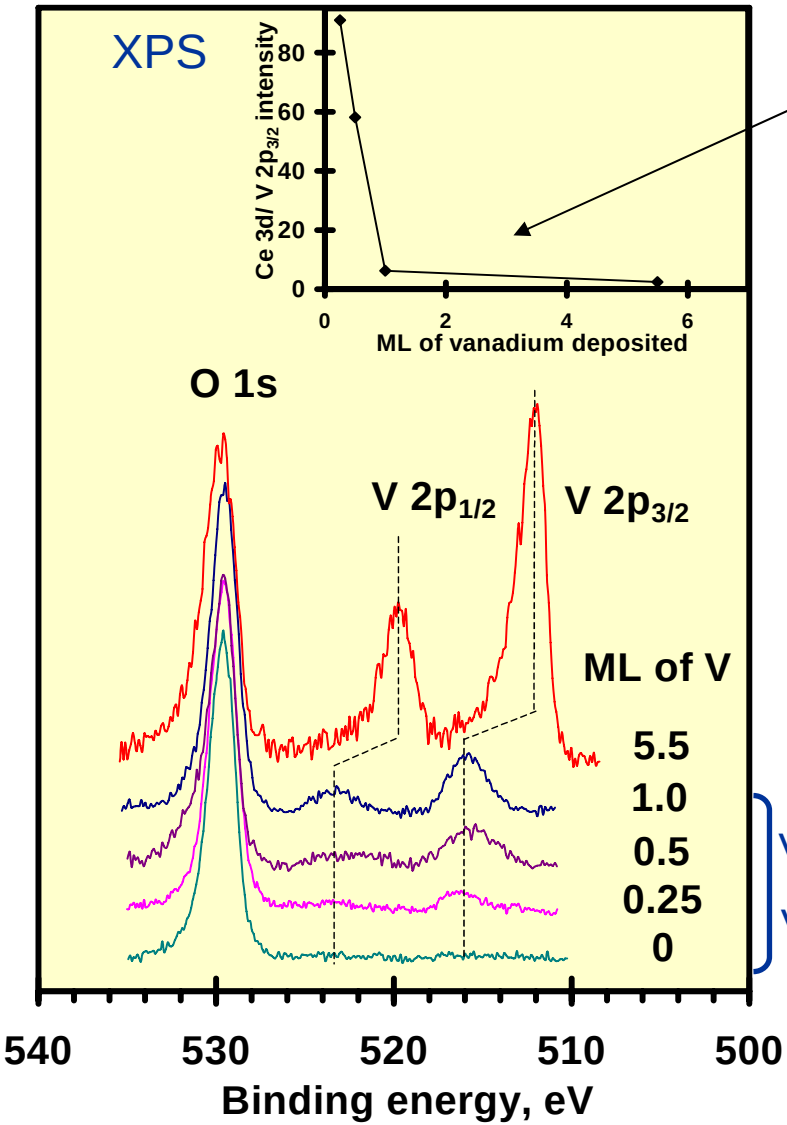

"Layer-by-layer" film growth

V^{+3}

V $2p_{3/2}$ = 515.7 eV

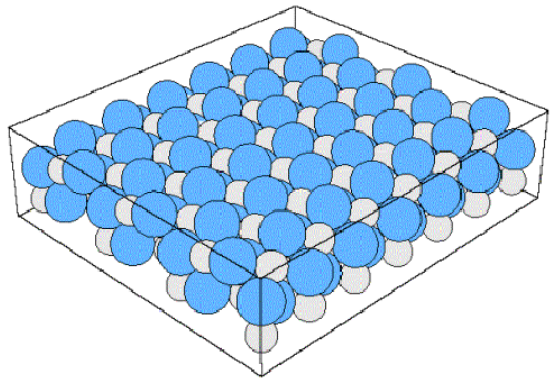

$CeO_2(111)$

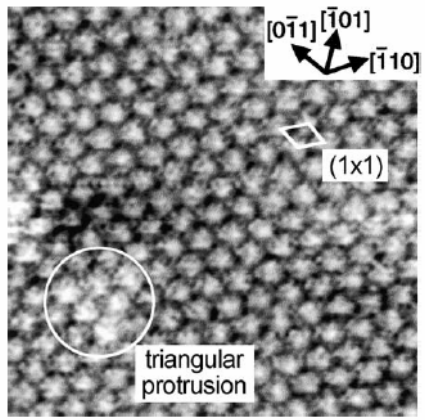

Atom-resolved NC-AFM image

Namai et al. *Catalysis Today* **85** (2003) 79.

Metal Oxide	ΔG_f^o kcal/mole of metal cation
V_2O_3	-136.2
V_2O_5	-169.7
CeO_2	-244.9
Ce_2O_3	-203.9
TiO_2	-212.6
Ti_2O_3	-171.4

	ΔG^o kcal/mole
$6\ CeO_2 + 2\ V \rightarrow V_2O_3 + 3\ Ce_2O_3$	-26.3
$10\ CeO_2 + 2\ V \rightarrow V_2O_5 + 5\ Ce_2O_3$	70.7
$6\ TiO_2 + 2\ V \rightarrow V_2O_3 + 3\ Ti_2O_3$	-25.1
$10\ TiO_2 + 2\ V \rightarrow V_2O_5 + 5\ Ti_2O_3$	72.7
$V_2O_3 + 4\ CeO_2 \rightarrow V_2O_5 + 2\ Ce_2O_3$	97.0
$V_2O_3 + 4\ TiO_2 \rightarrow V_2O_5 + 2\ Ti_2O_3$	97.8

0.5 ML VO_x - XPS

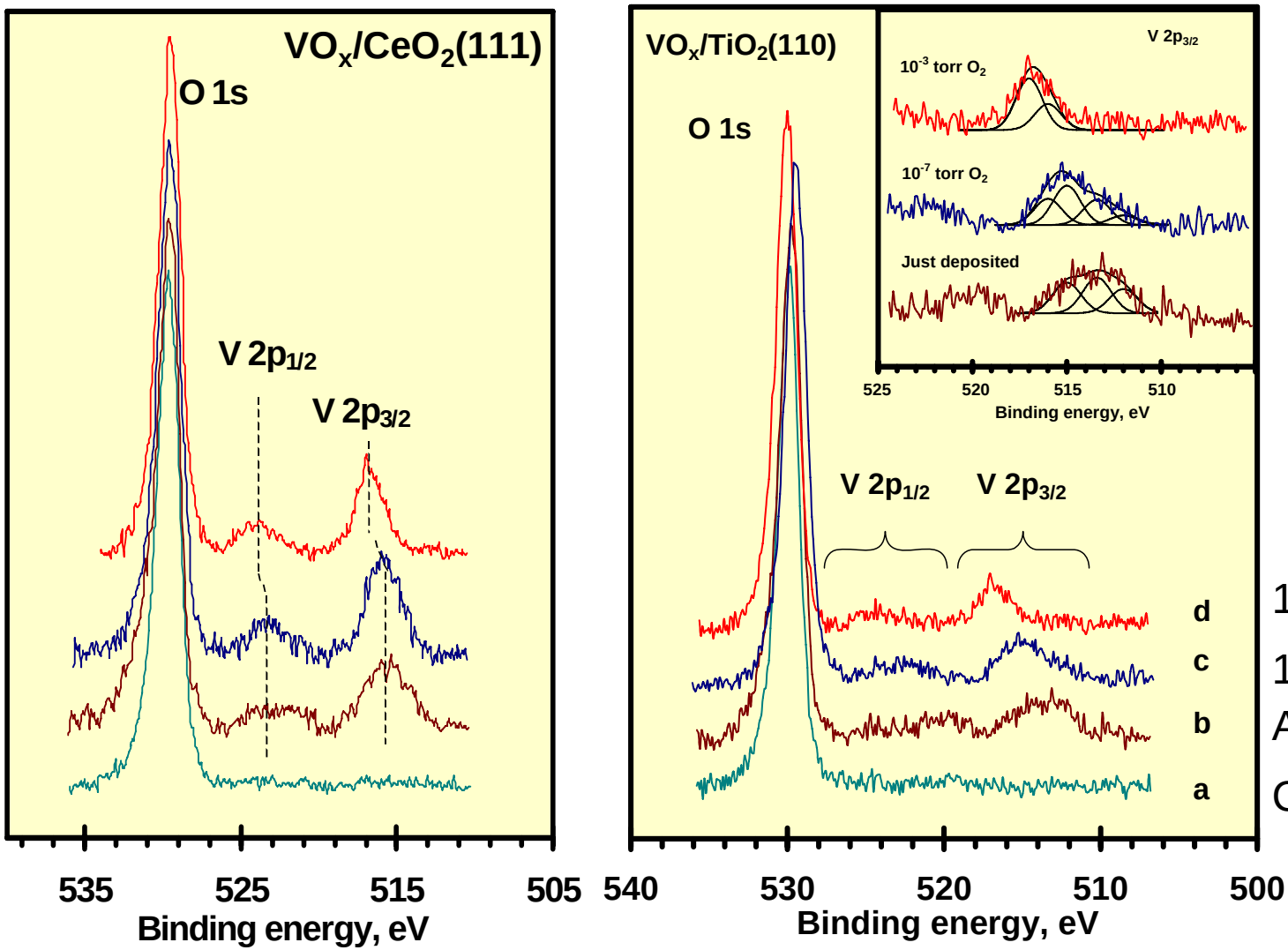

V $2p_{3/2}$	
V^0	512.3 eV
V^{+3}	515.3 eV
V^{+4}	515.7 eV
V^{+5}	516.8 eV

10^{-3} torr O_2 400 K

10^{-7} torr O_2 575 K

As deposited

Clean substrate

XPS – 0.5 ML Vanadia/CeO_2(111)

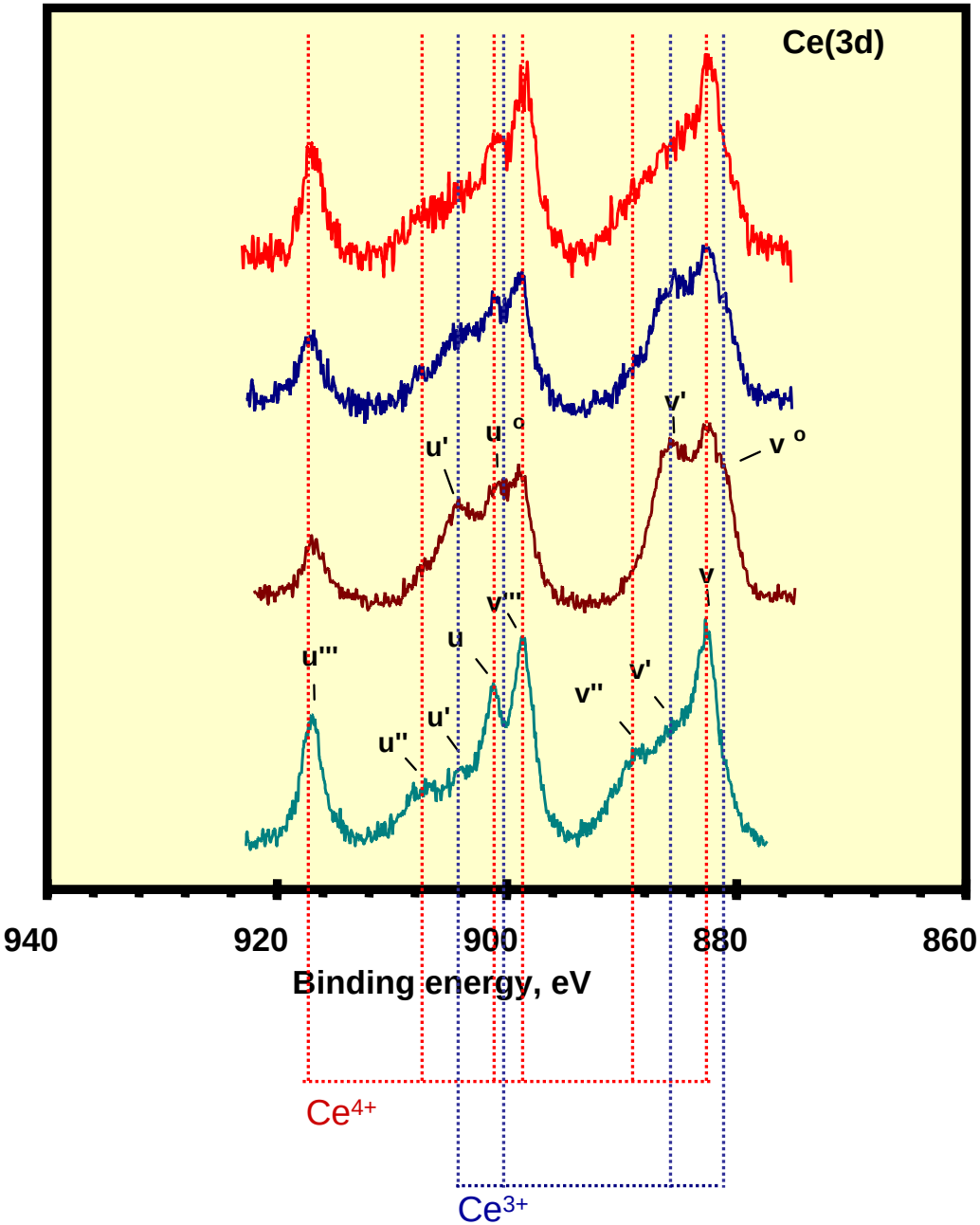

10^{-3} torr O_2, 400K

10^{-5} torr O_2, 400K

0.5 ML V as deposited

CeO_2(111)

	Peaks	Initial State	Final State
Ce^{3+}	v^o,u^o	$3d^{10}4f^1$	$3d^94f^2V^{n-1}$
Ce^{3+}	v',u'	$3d^{10}4f^1$	$3d^94f^0V^n$
Ce^{4+}	v,u	$3d^{10}4f^0$	$3d^94f^2V^{n-2}$
Ce^{4+}	v'',u''	$3d^{10}4f^0$	$3d^94f^1V^{n-1}$
Ce^{4+}	v''',u'''	$3d^{10}4f^0$	$3d^94f^0V^n$

Thermal Stability of $V_2O_5/CeO_2(111)$

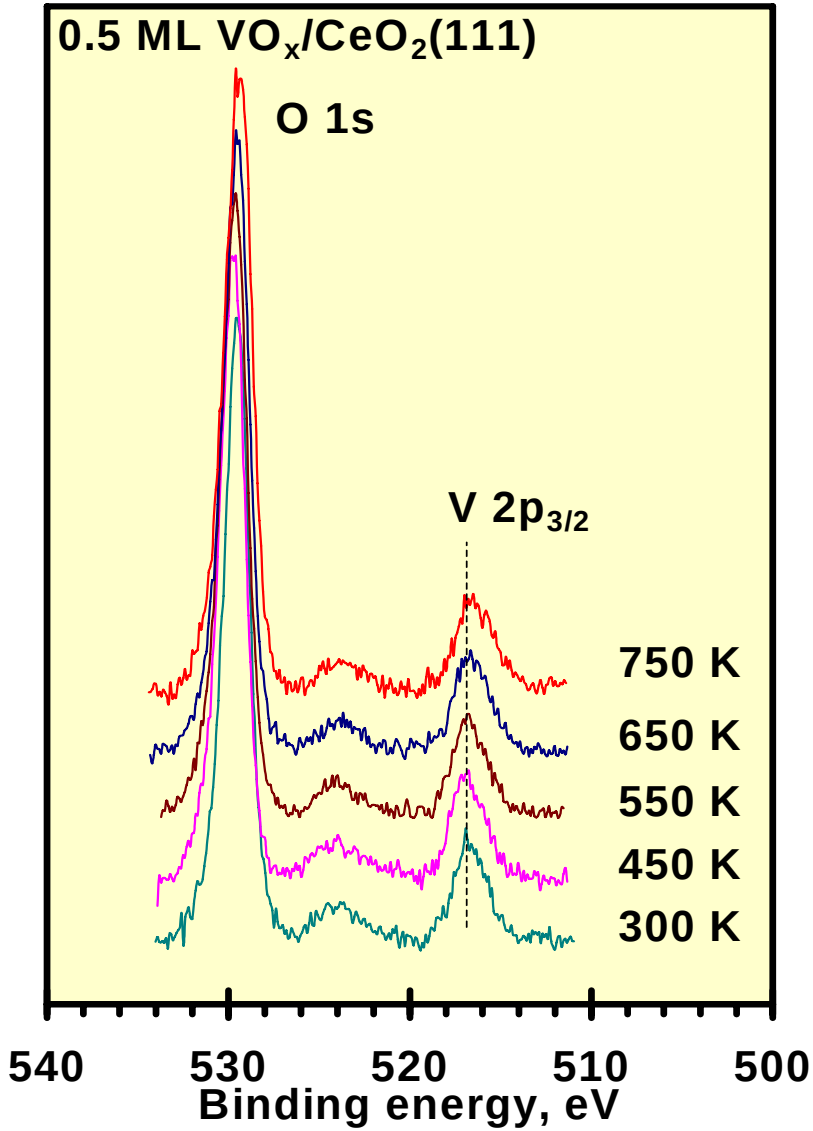

Reduction is evident at T ≥ 650 K

Summary of Film Growth Characterization

- "Layer-by-Layer" vanadia film growth on $CeO_2(111)$, $TiO_2(110)$, and $ZrO_2(110)$.
- The oxidation state of the vanadium cations in monolayer films can be varied from +3 to +5
- Unable to grow multilayer films of V_2O_5 on $CeO_2(111)$ and $TiO_2(110)$ in UHV

Temperature Programmed Desorption (TPD)

- E_a and A for for desorption and surface reaction
- Surface-adsorbate bonding
- Structure of adsorbed intermediates
- Reaction pathways and mechanisms

Procedure

- Dose reactant at low temperature
- Heat sample with a linear temperature ramp
- Monitor desorbing species with mass spec

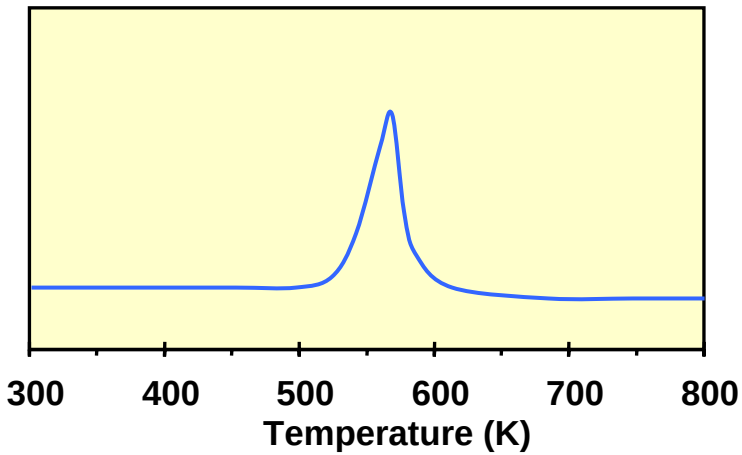

CH_3OH TPD 0.5 ML $V_2O_5/CeO_2(111)$

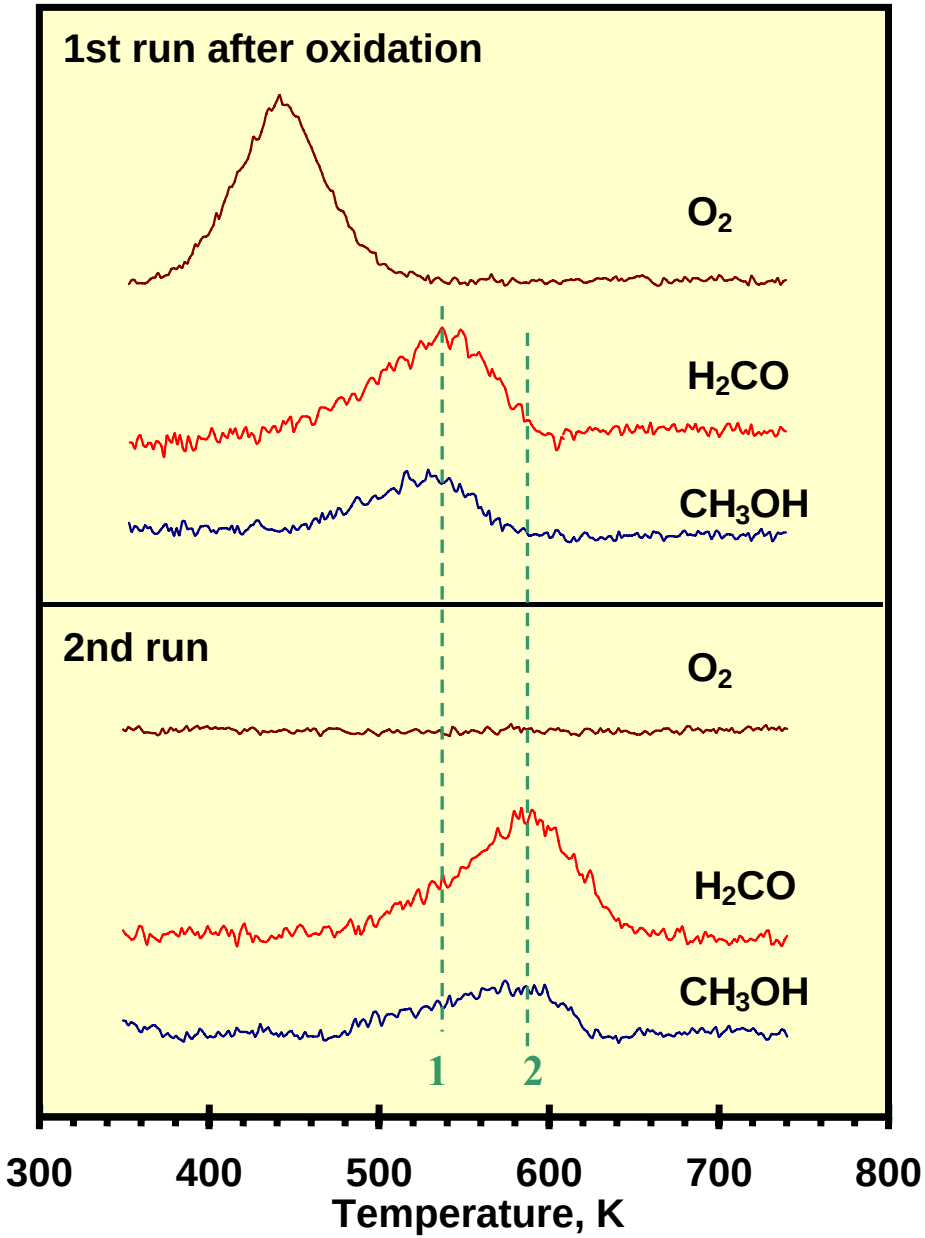

$E_{a,1}$ ~ 140 kJ/mole

$E_{a,2}$ ~ 155 kJ/mole

E_a for C-H bond cleavage from adsorbed methoxides is much greater than E_{app} for high surface area catalysts.

Kinetic Isotope Effect

CH_3OH/CD_3OD TPD

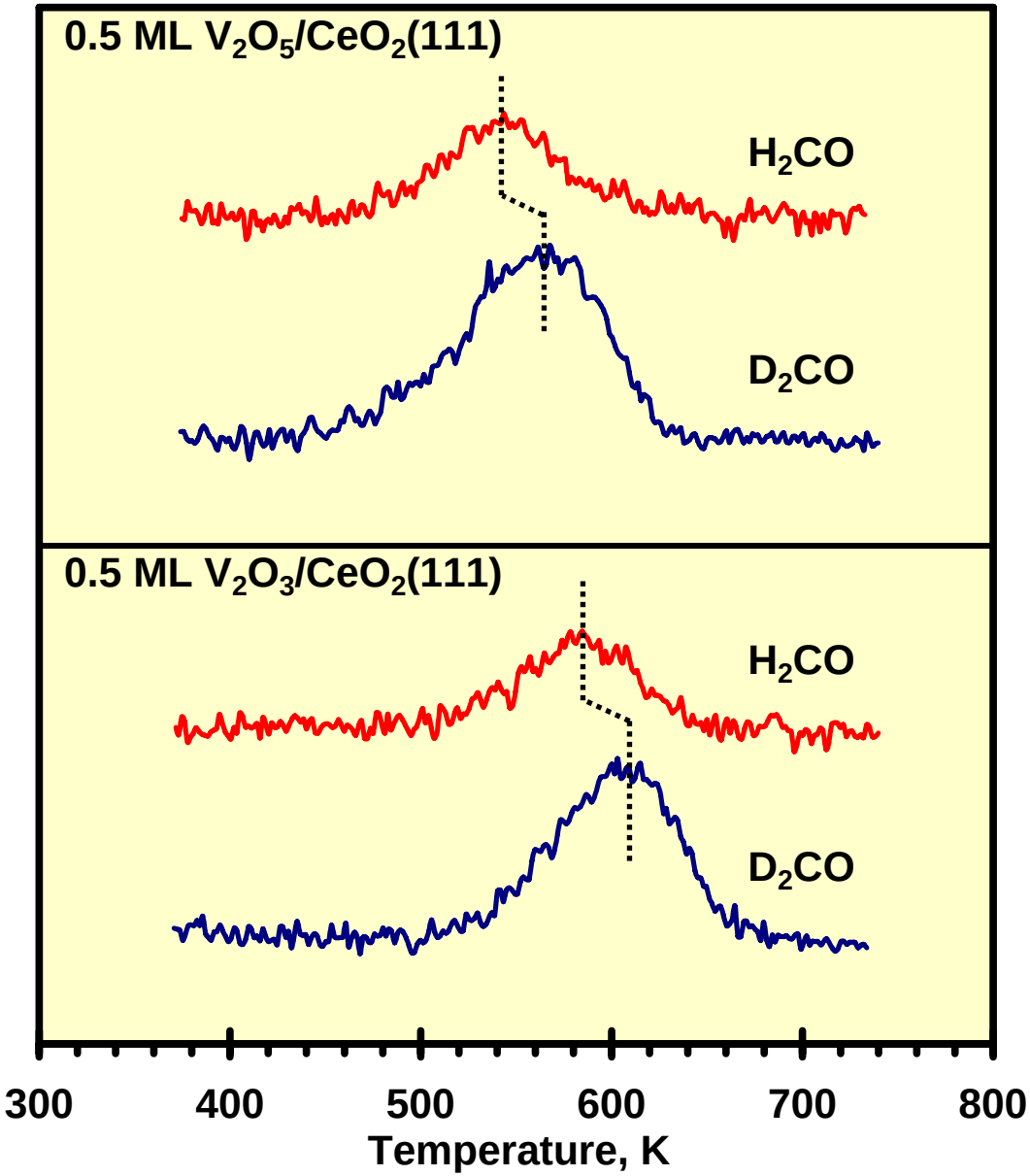

C-H bond cleavage is rate limiting step on both V^{+5} and V^{+3}

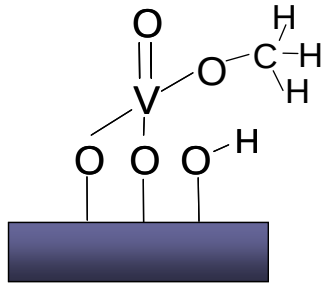

$H_2CO + H_2O$

0.5 ML $VO_x/CeO_2(111)$ - CH_3OH TPD

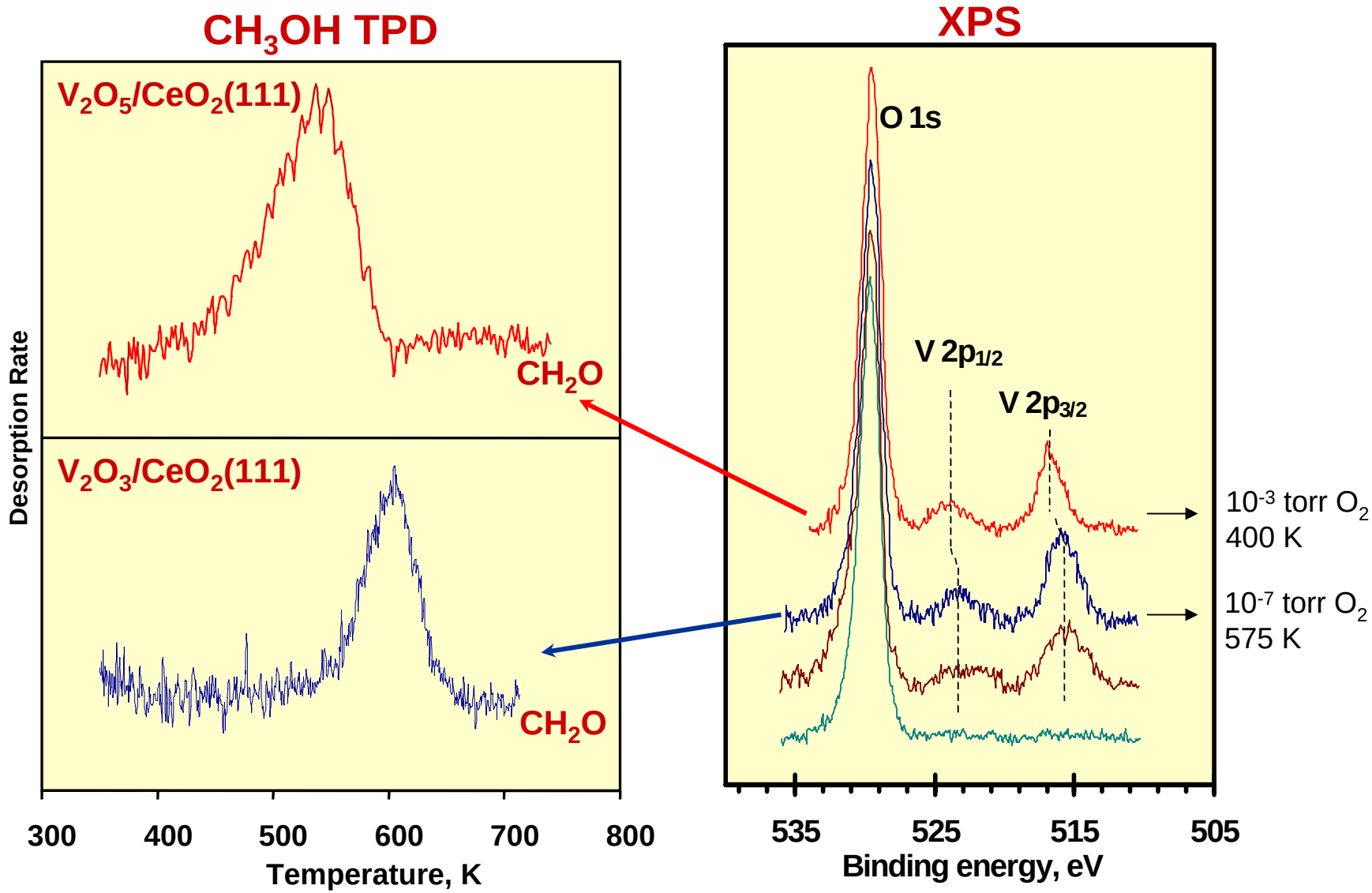

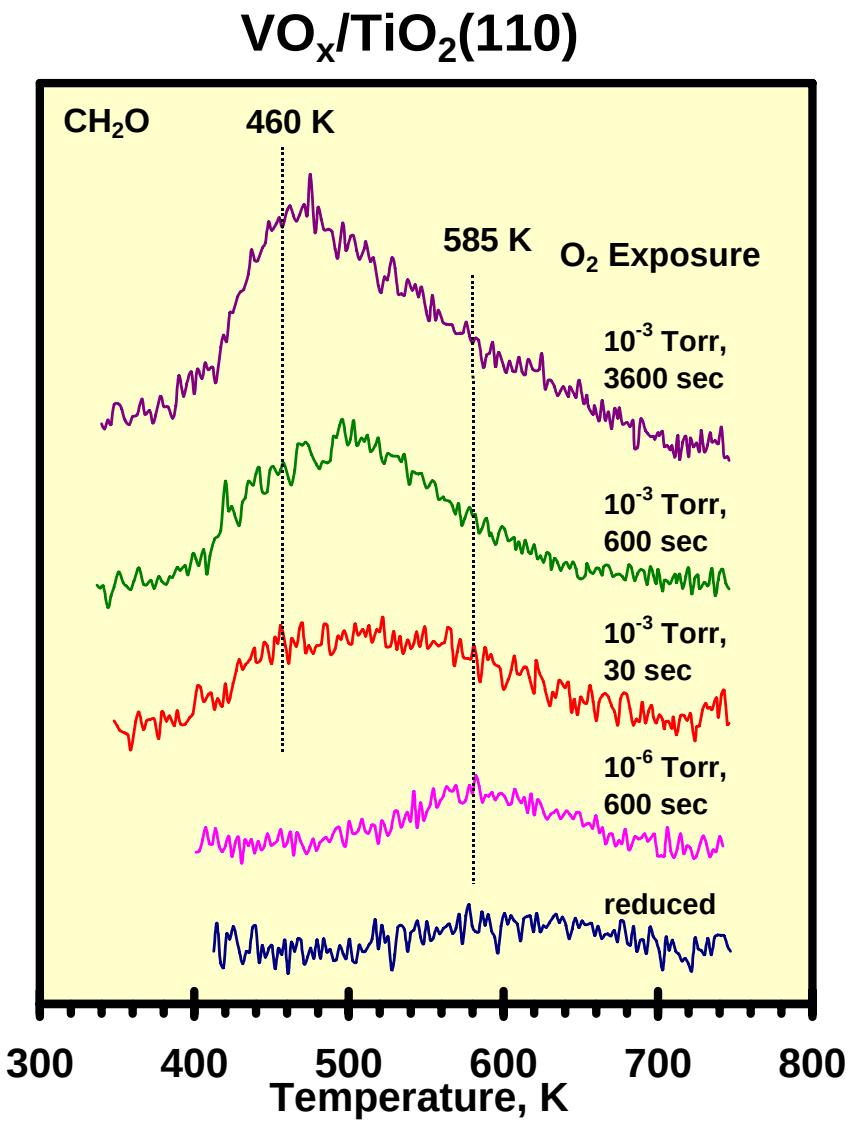
VOx/TiO2(110)
CH2O
460 K
585 K
O2 Exposure
10-3 Torr, 3600 sec
10-3 Torr, 600 sec
10-3 Torr, 30 sec
10-6 Torr, 600 sec
reduced
300
400
500
600
700
800
Temperature, K

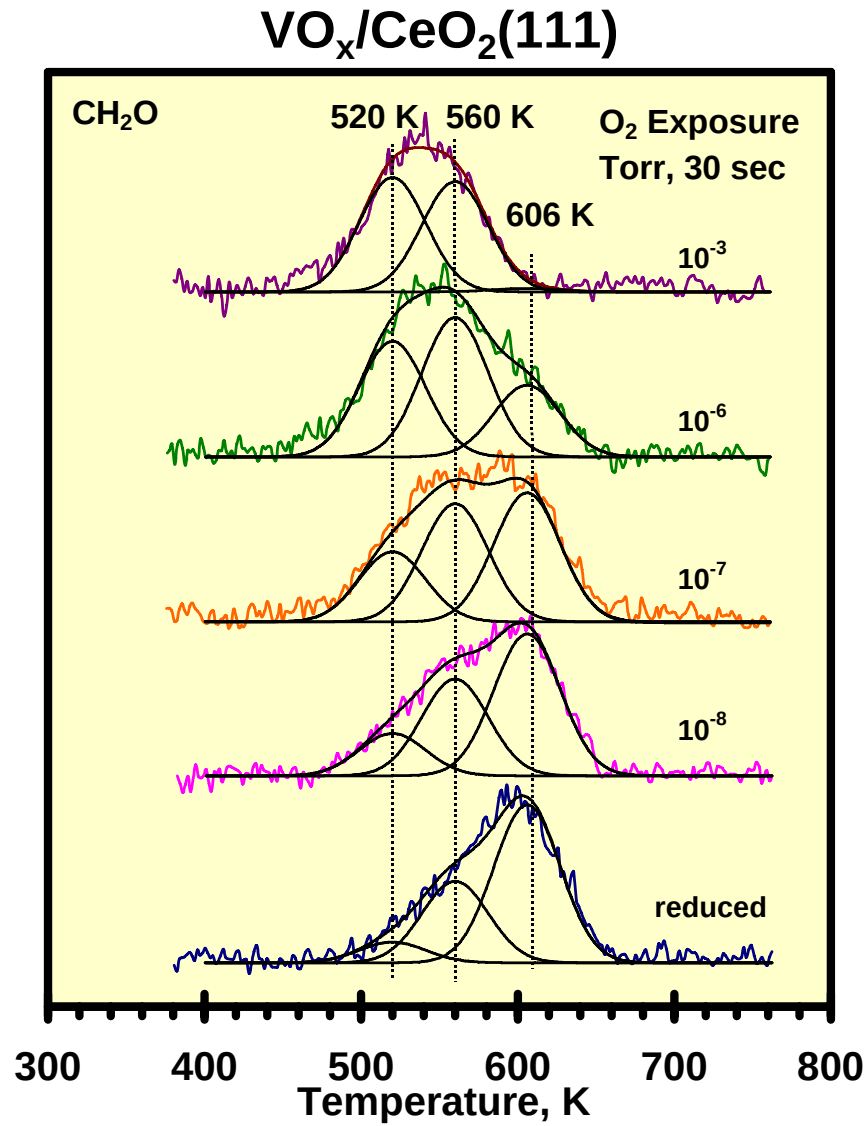
VOx/CeO2(111)
CH2O
520 K
560 K
606 K
O2 Exposure
Torr, 30 sec
10-3
10-6
10-7
10-8
reduced
300
400
500
600
700
800
Temperature, K

Summary of Activation energies

$V*\text{-}OCH_3 \rightarrow CH_2O + V*\text{-}H$

Model Catalysts

	V_2O_3	V_2O_5
$TiO_2(110)$	~160 kJ/mole	120 kJ/mole
$ZrO_2(110)$	158 kJ/mole	124 kJ/mole
$CeO_2(111)$	155 kJ/mole	140 kJ/mole

High surface area catalysts Catalysts

Catalyst (monolayer vanadia coverage)	TOF for CH_3OH Oxidation to H_2CO (s^{-1})	Apparent E_a (kJ/mol)
25 % V_2O_5/Al_2O_3	0.068	83.7
7 % V_2O_5/Nb_2O_5	0.4	71.1
6 % V_2O_5/TiO_2	1.1	92.0
4 % V_2O_5/ZrO_2	1.7	75.3
3 % V_2O_5/CeO_2	10.0	83.7

V_2O_5/CeO_2 - Powder Samples - CH_3OH TPD

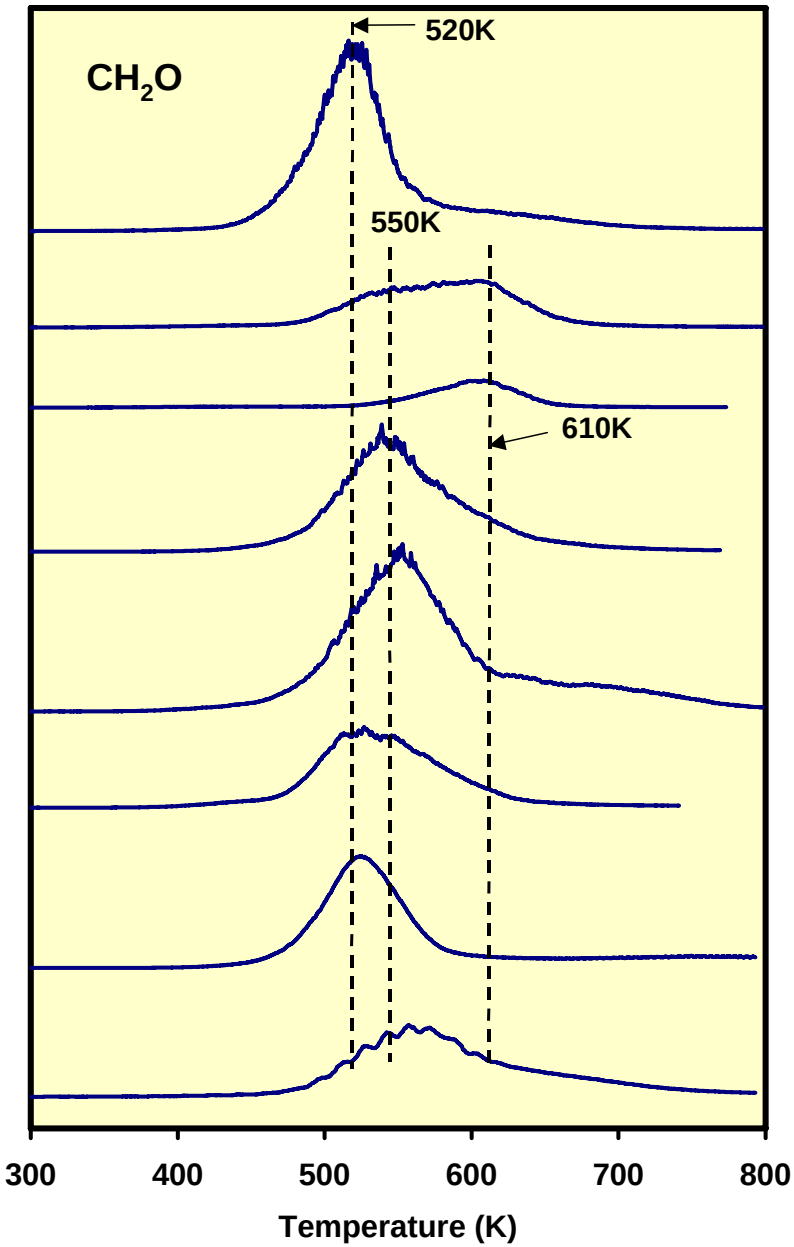

Fresh Sample – fully oxidized

Slightly reduced

Highly reduced

<u>Reoxidation treatment</u>

0.1 Torr O_2, 300 K

0.1 Torr O_2, 525 K

0.1 Torr O_2, 750 K

1.0 Torr O_2, 750 K

Reduced by annealing at 750 K in vacuum

High Surface Area V_2O_5/CeO_2 catalyst

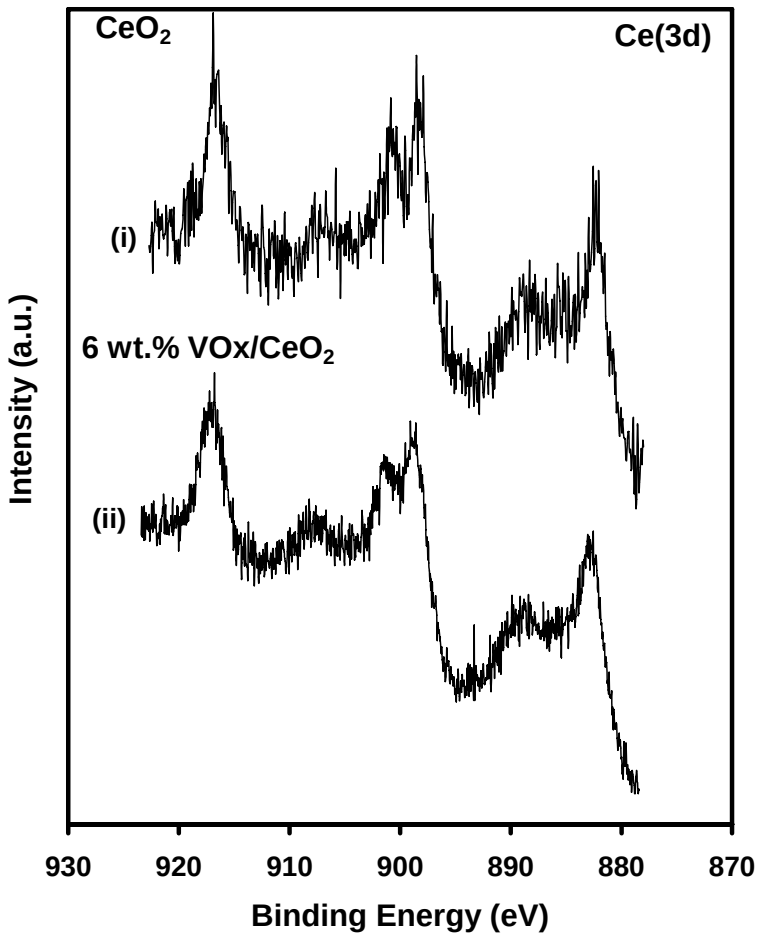

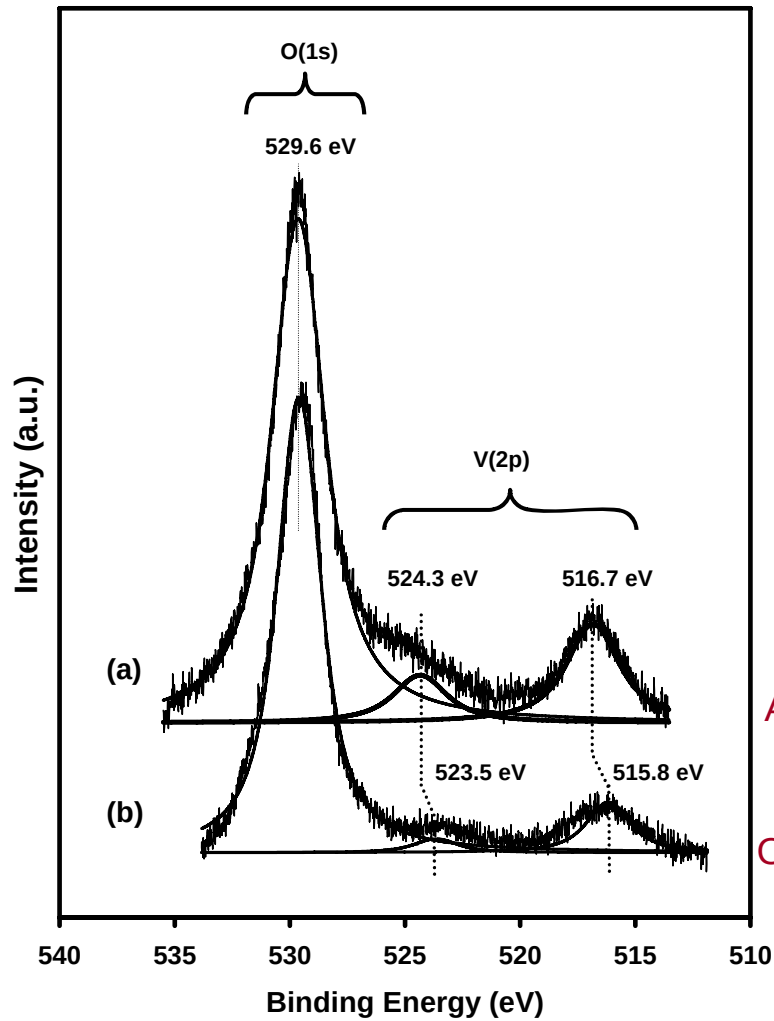

After CH_3OH TPD

Oxidized sample

Single Crystal Model Systems
Summary

- Reactivity trends are consistent with those of high surface area analogues
  - Monolayer vanadia films are active for the oxidation of methanol to formaldehyde
  - Multilayer films are inactive
- Activation energy for the dehydrogenation of methoxide to produce formaldehyde is a function of the oxidation state of the vanadium cations
- Methanol can be used as a chemical probe of the vanadium oxidation state.

Three-Way Automotive Emissions Control Catalysts

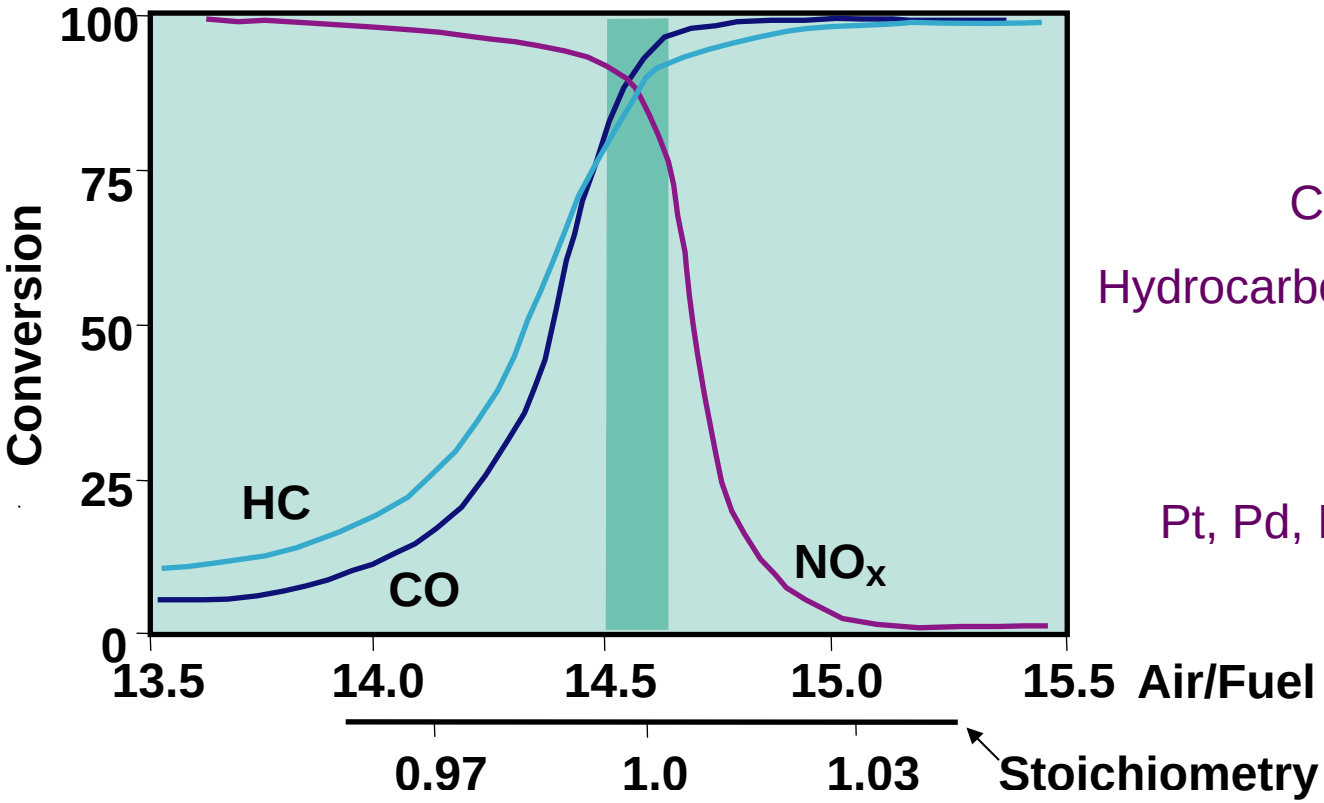

Reactions

$CO + O_2 \rightarrow CO_2$

Hydrocarbons + $O_2 \rightarrow CO_2 + H_2O$

$NO_x \rightarrow N_2$

Catalysts

Pt, Pd, Rh - CeO_2, ZrO_2, La_2O_3

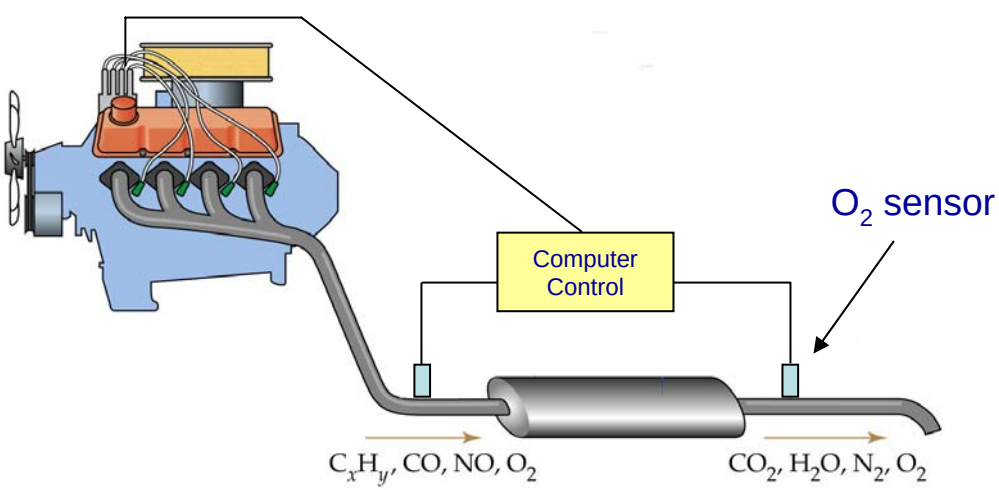

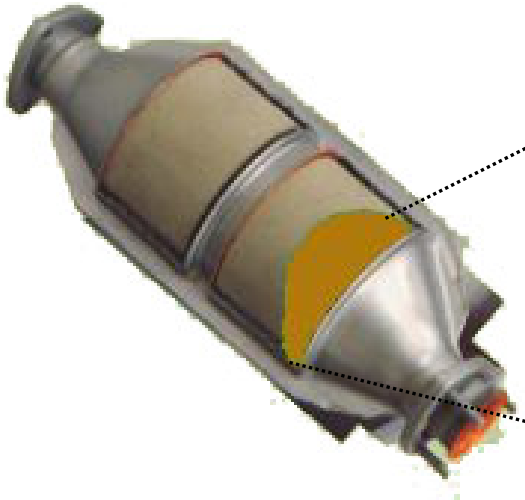

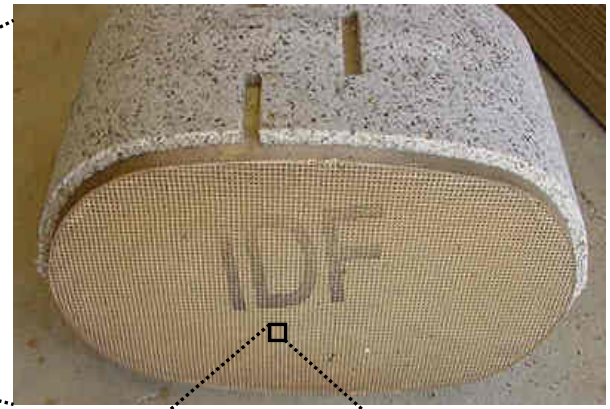

Dense Alumina Monolith

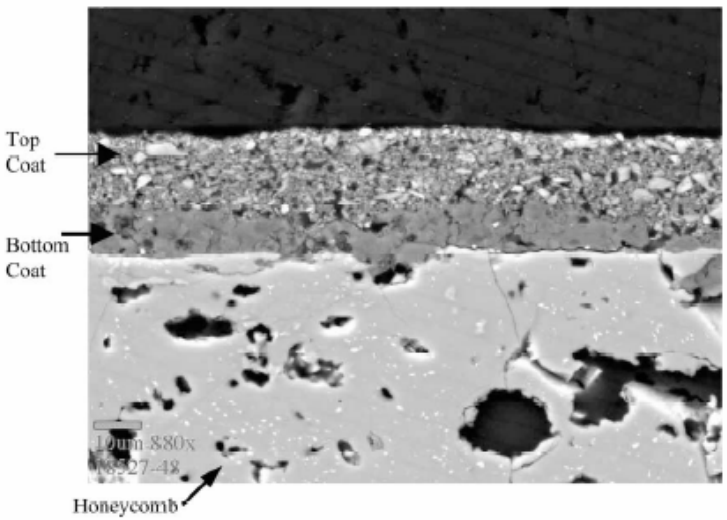

Porous Alumina Washcoat

Impregnated with:

CeO_2, ZrO_2, La_2O_3

Rh, Pd, Pt

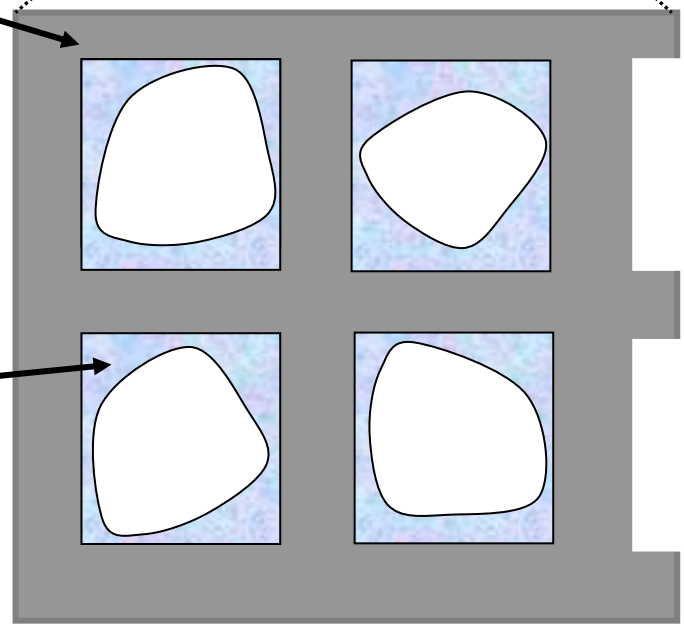

Issues in Automotive Catalysis

- Tighter emissions standards require better catalysts
- Cold start emissions
  - Close-coupled converter
  - Thermal stability
- Sulfur tolerance
- Durability
- NO_x reduction for lean burn engines

Role of Ceria and Zirconia in Automotive Emissions Control Catalysts

CeO_2

- Enhance activity for water gas shift reaction
- Stabilization of metal dispersion
- Stabilization of γ-Al_2O_3 support
- Enhance metal reactivity
- Provide oxygen storage capacity

ZrO_2

- Stabilization of CeO_2 dispersion
- Enhance CeO_2 oxygen storage capacity

Ceria – Zirconia Interfaces

Fundamental question: How do interactions at the ceria-zirconia interface influence the redox and catalytic properties of ceria?

Experimental Approach:

- Model systems consisting of metal oxide single crystals and thin films supported on metal oxide single crystals
- Kinetic measurements
- Surface-sensitive spectroscopic probes
- Microscopy

Model Systems Studied

CeO_2(100)	CeO_2(111)
CeO_2/ZrO_2 (100)	CeO_2/ZrO_2 (110)
CeO_2/ZrO_2 (111)	CeO_2/Al_2O_3(0001)

Model Catalysts

Oxide Single Crystals

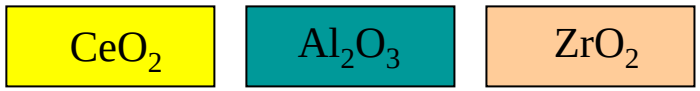

Ceria Thin-Films

Oxide-supported Rh particles

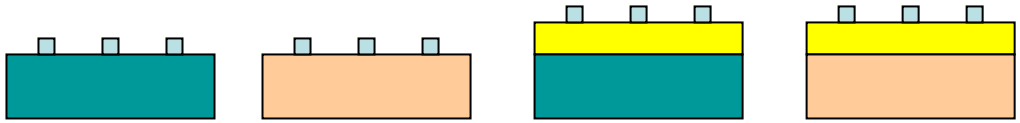

Film Growth

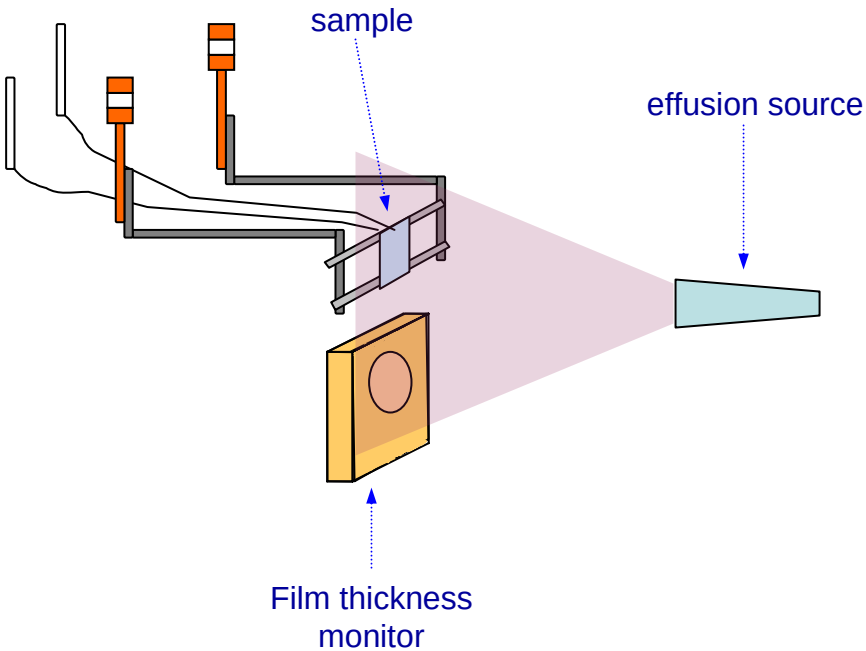

Model Catalysts

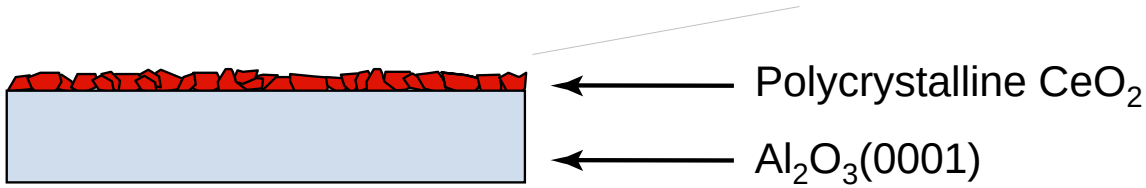

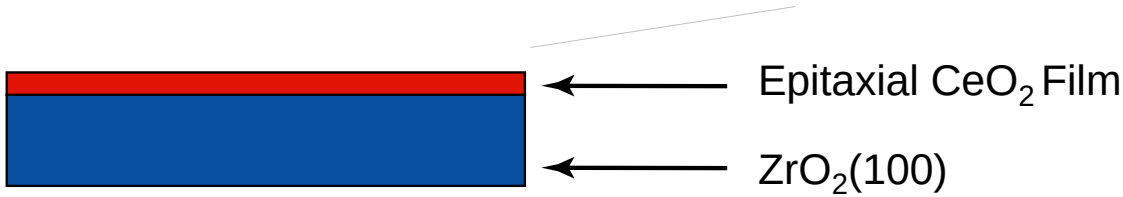

$CeO_2(111)$ - CH_3OH TPD

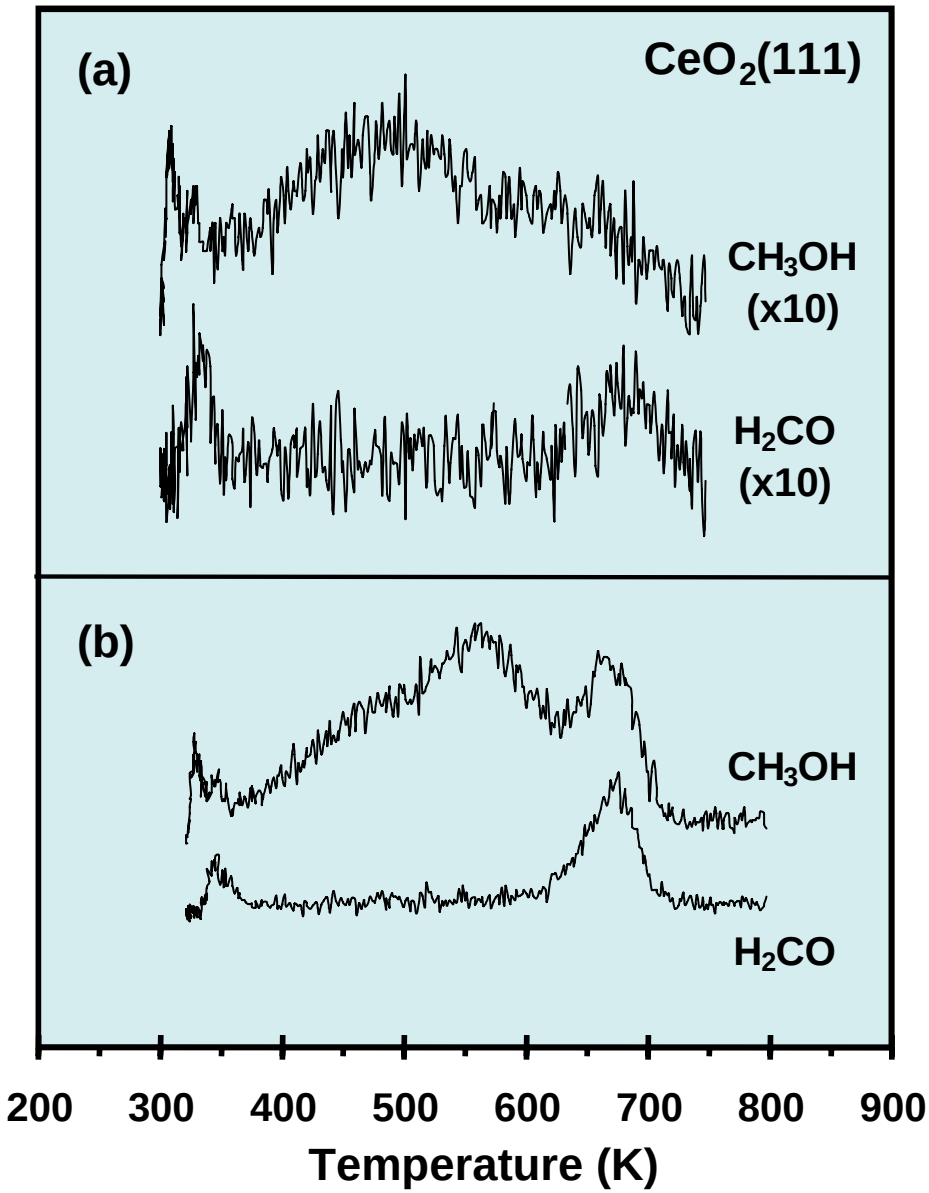

Vacuum Annealed
(nearly stoichiometric)

Ar^+ Sputtered
(reduced)

$CeO_2/\alpha\text{-}Al_2O_3(0001)$ CH_3OH TPD

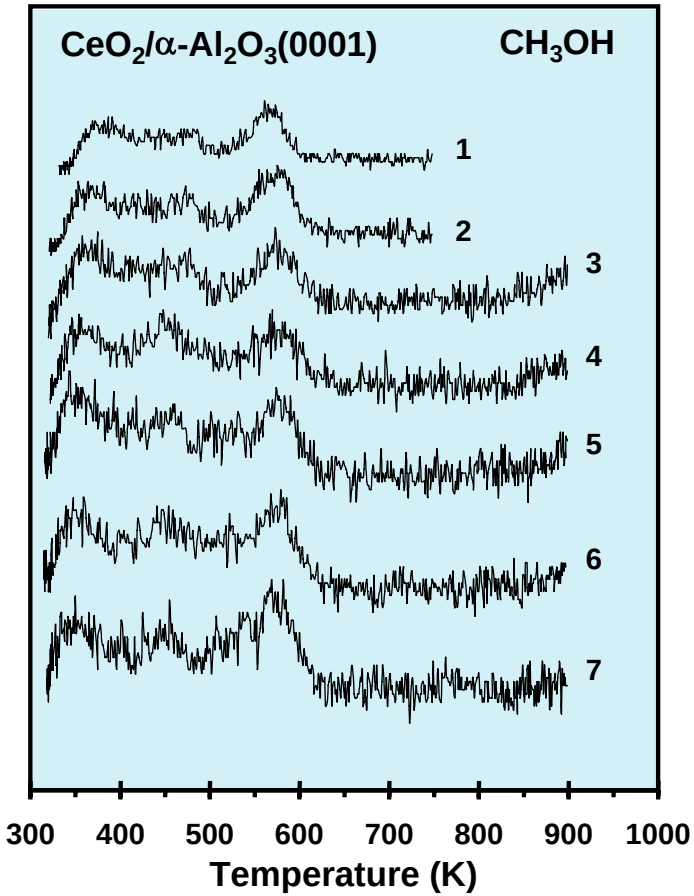

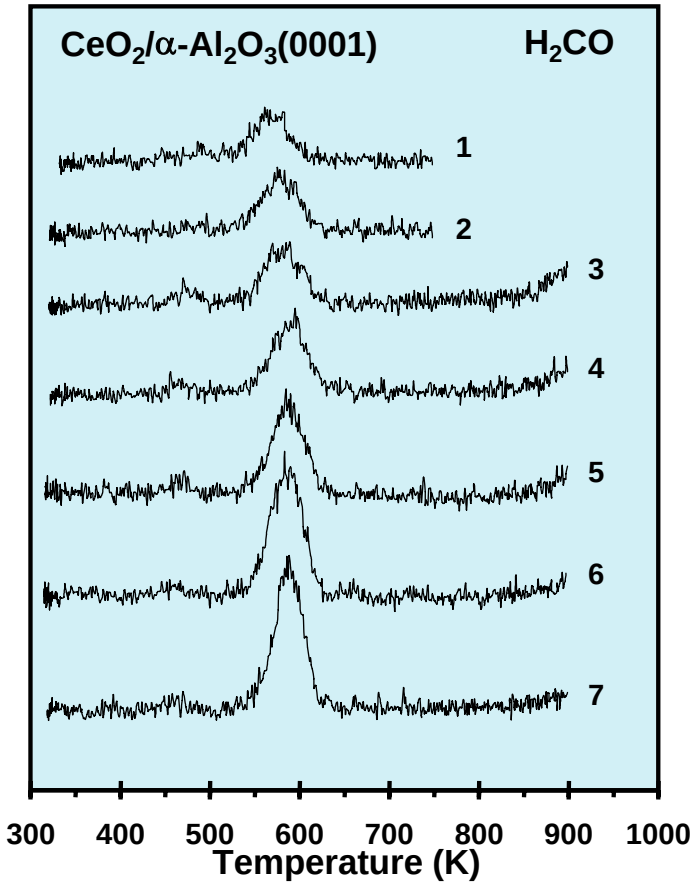

Results similar to those obtained for $CeO_2(111)$

- Dissociative adsorption of CH_3OH on surface oxygen vacancies
- Concentration of oxygen vacancies increases with each TPD run
- Annealing temperature does not affect properties

CeO_2/YSZ(100) CH_3OH TPD

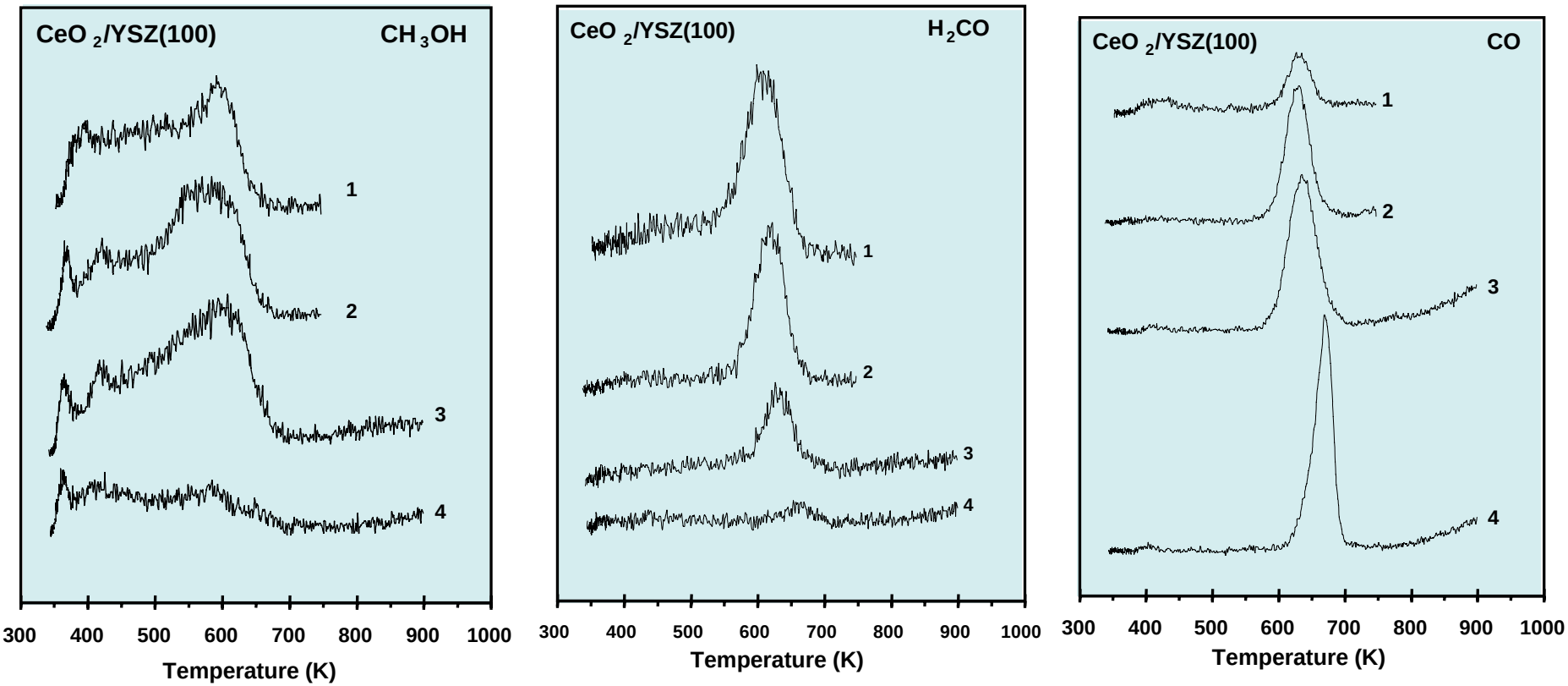

- High oxygen vacancy concentration in O_2 annealed epitaxial ceria film
- Heating to 900 K causes significant reduction of the ceria film?

X-ray Photoelectron Spectroscopy - XPS

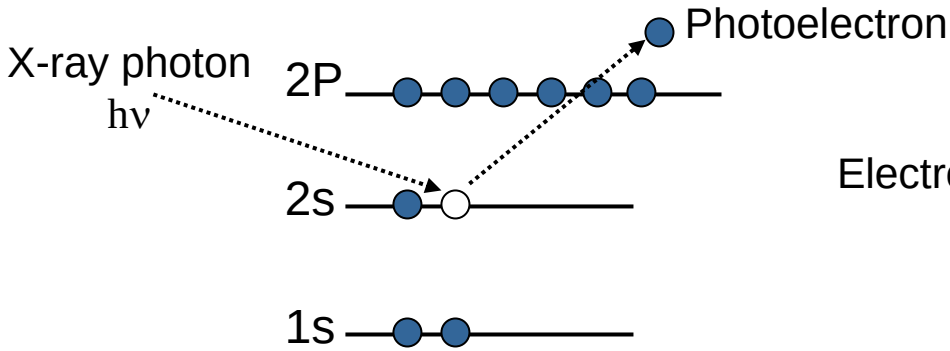

Electron Binding Energy = $h\nu - E_{KE} - \Psi$

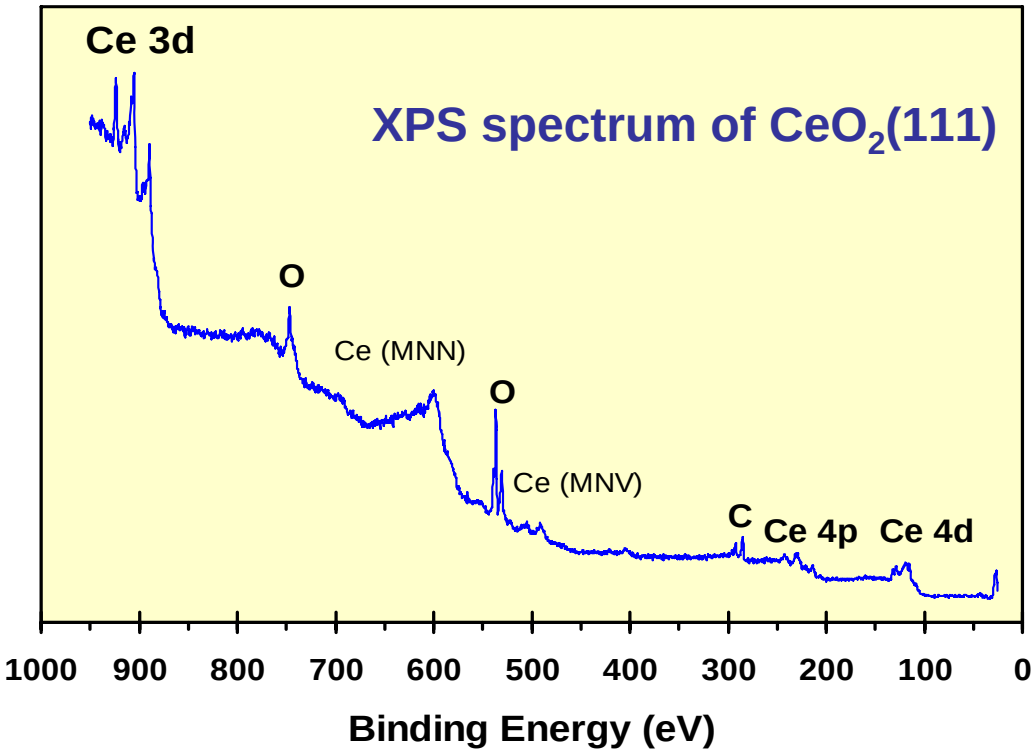

- Surface composition
- Morphology and thickness of thin films
- Oxidation states
- Adsorbate structure

XPS: Thermal Stability of Ceria Films

CeO_2 / α-Al_2O_3(0001)

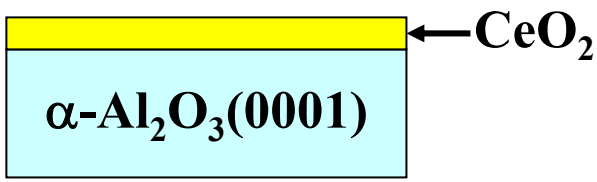

CeO_2 / ZrO_2(100)

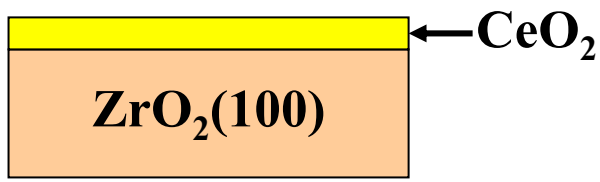

XPS: Ce 3d

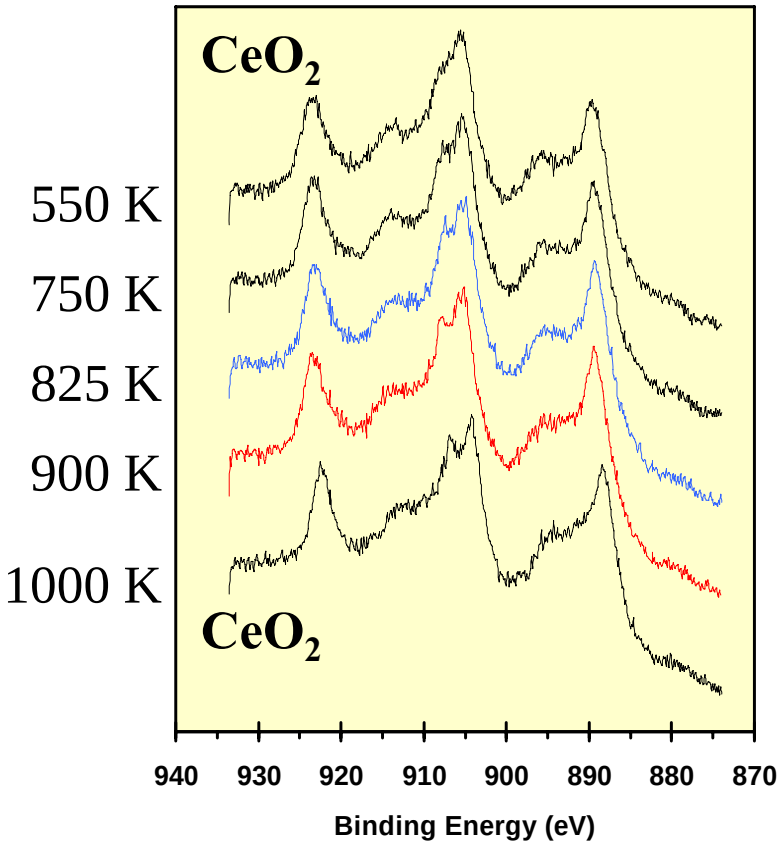

XPS: Ce 3d

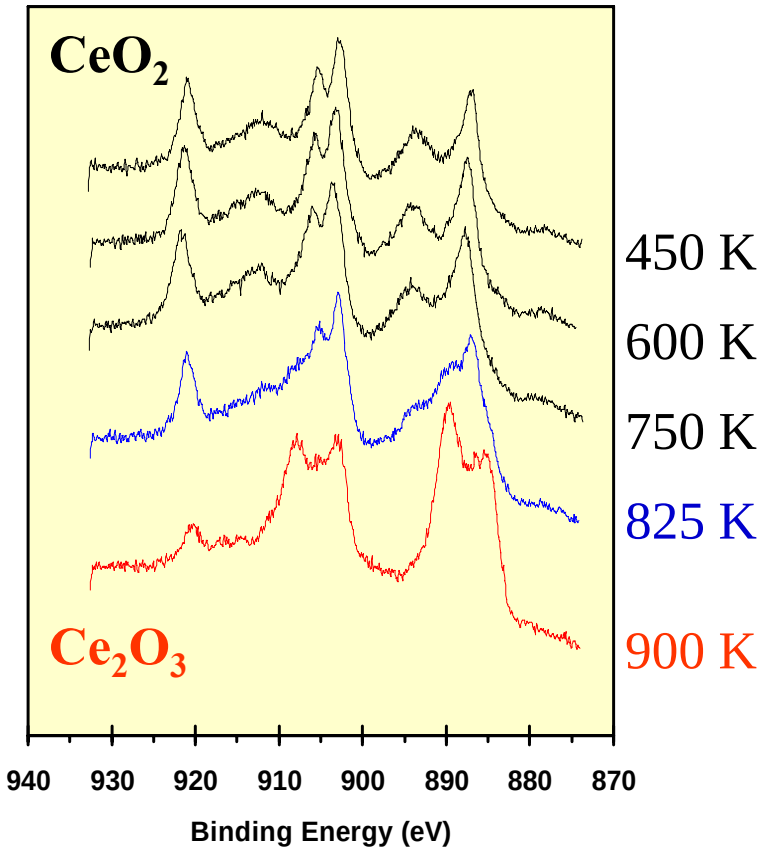

Ceria/Zirconia

Results from Pulsed Neutron Diffraction Studies

Mamontov, Egami et al., J. Phys. Chem. B 104 (2000) 11110.

○ - Oxygen vacancies

● - Oxygen interstitials

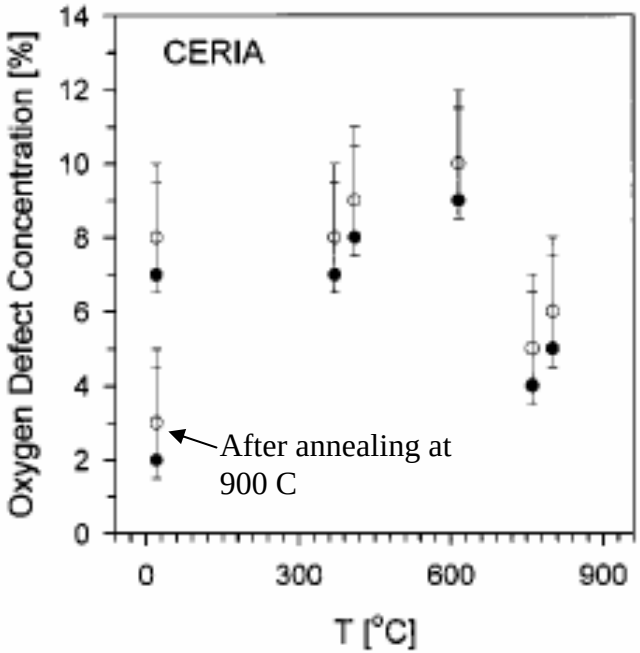

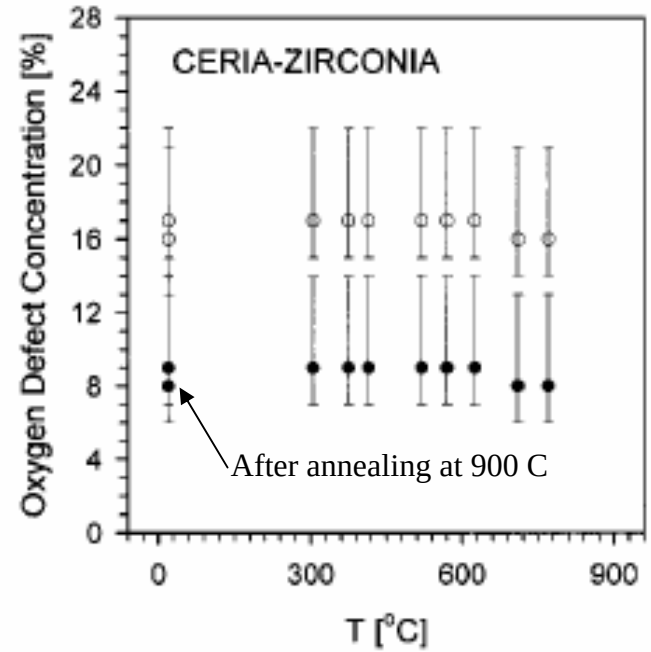

- Ceria sample is nearly stoichiometric
- Ceria-zirconia sample is oxygen deficient
- CeO_2 oxygen vacancy-interstitial defect concentration decreases upon heating to 700ºC

Enhanced Reducibility of CeO_2/ZrO_2

$$4CeO_2 \longleftrightarrow 2Ce_2O_3 + O_2$$

- Bulk Thermodynamics: T_{red} ~ 1300 K
- TPD & XPS Results: T_{red} ~ 750 to 900 K

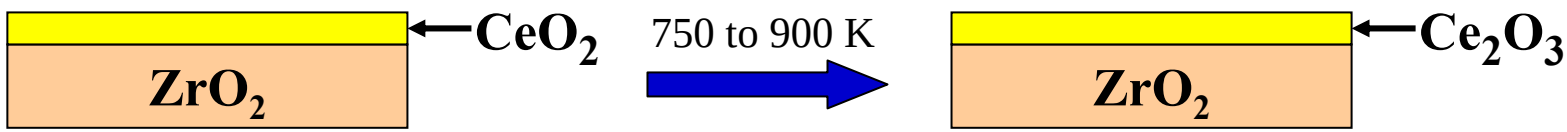

- Lattice mismatch at interface maintains small ceria grain size

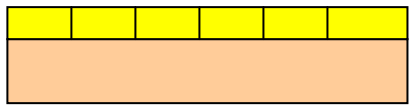

a = 5.4 Å

a = 5.1 Å

Ceria grain size ~75 Å

- Bonding at interface prevents CeO_2 phase transformation

ZrO_2, CeO_2 – cubic fluorite

Ce_2O_3 – trigonal

Ce_2O_3/ZrO_2, – cubic fluorite?

- Interfacial strain alters vacancy and interstitial concentrations in CeO_2

Steam Reforming of Methanol

$$CH_3OH + H_2O \rightarrow CO_2 + 3\,H_2$$

- Cu/ZnO is used commercially

  Has high activity and selectivity but

  - Cu sinters at T>575 K
  - Pyrophoric once reduced

- Pd/ZnO has been proposed as an alternative catalyst

  Has high activity and selectivity

  Structure-activity relationships are poorly understood

CH_3OH Oxidation on ZnO(0001) TPD – Pathways and Intermediates

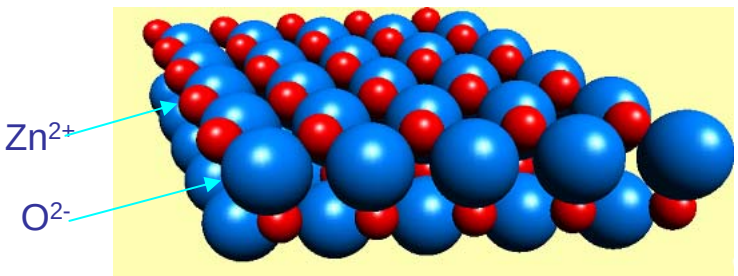

ZnO(0001)

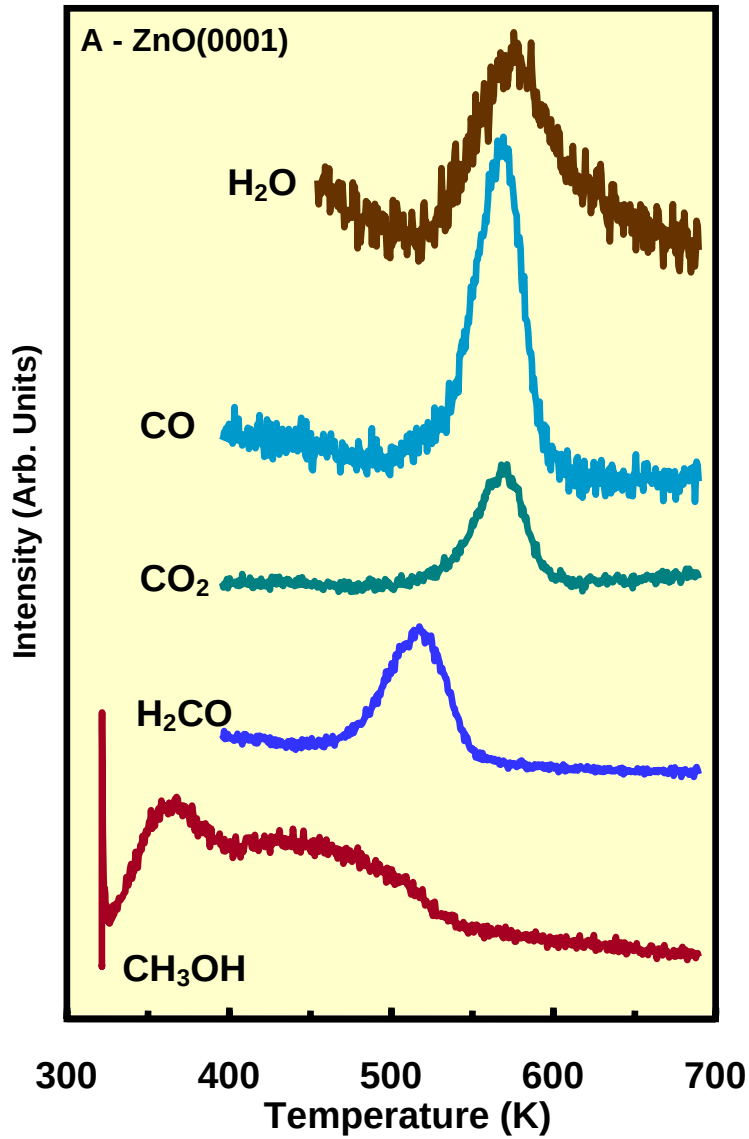

CH_3OH Oxidation on ZnO(0001) TPD – Pathways and Intermediates

>150 K	$CH_3OH(g) \rightarrow CH_3O(ad) + H(ad)$
> 400 K	$CH_3O(ad) + O(l) \rightarrow HCOO(ad) + 2\,H(ad)$
510-530 K	$CH_3O(ad) \rightarrow CH_2O(g) + H(ad)$
560-580 K	$HCOO(ad) \rightarrow CO_2(g) + H(ad)$
	$HCOO(ad) \rightarrow CO\,(g) + OH(ad)$
	$2\,OH(ad) \rightarrow H_2O(g) + O(l)$

CH_3OH Oxidation on ZnO(0001) TPD – Pathways and Intermediates

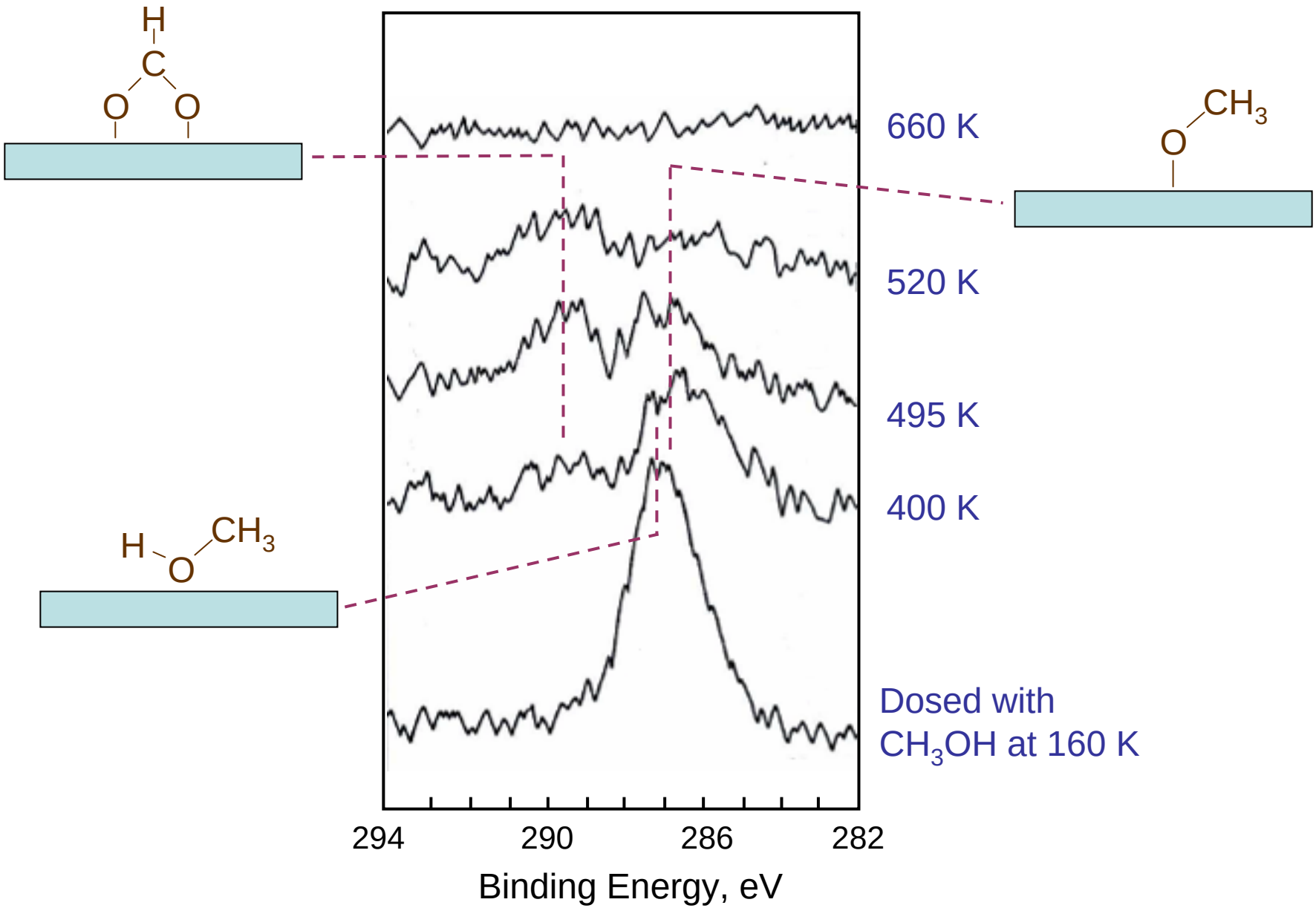

Methanol Steam Reforming

N. Iwasa et al. / Applied Catalysis A: General 125 (1995) 145–157

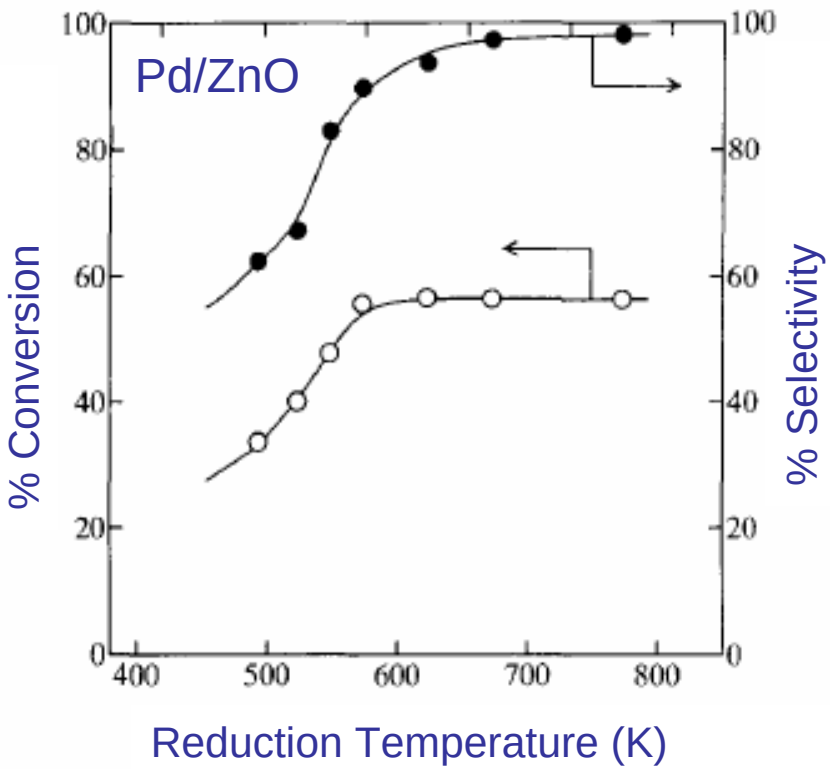

10.1 kPa CH_3OH

10.1 kPa H_2O

493 K

$$\text{Selectivity} = \frac{CO_2}{CO + CO_2}$$

Methanol Dehydrogenation

N. Takezawa, N. Iwasa / Catalysis Today 36 (1997) 45–56

Table 4
Dehydrogenation of methanol over various supported Pd catalysts [a]

Catalyst [b]	Rate of H_2 production (μmol (min g-cat)$^{-1}$)	Selectivity (%)	
		CO	$HCOOCH_3$
Pd	192	100	0
Pd/SiO_2	17.6	100	0
Pd/MnO_2	74.5	100	0
Pd/MgO	101	100	0
Pd/Cr_2O_3	83.8	100	0
Pd/TiO_2	106	100	0
Pd/ZrO_2	188	100	0
Pd/HfO_2	59.3	100	0
Pd/La_2O_3	50	100	0
Pd/Nd_2O_3	142	100	0
Pd/ZnO	110	20	80

[a] Reaction temperature 473 K: $P(CH_3OH) = 10.1$ kPa.
[b] Metal loading, 1.0 wt.%.

Steam Reforming of Methanol – Pd/ZnO

N. Iwasa et al. / Applied Catalysis A: General 248 (2003) 153–160 155

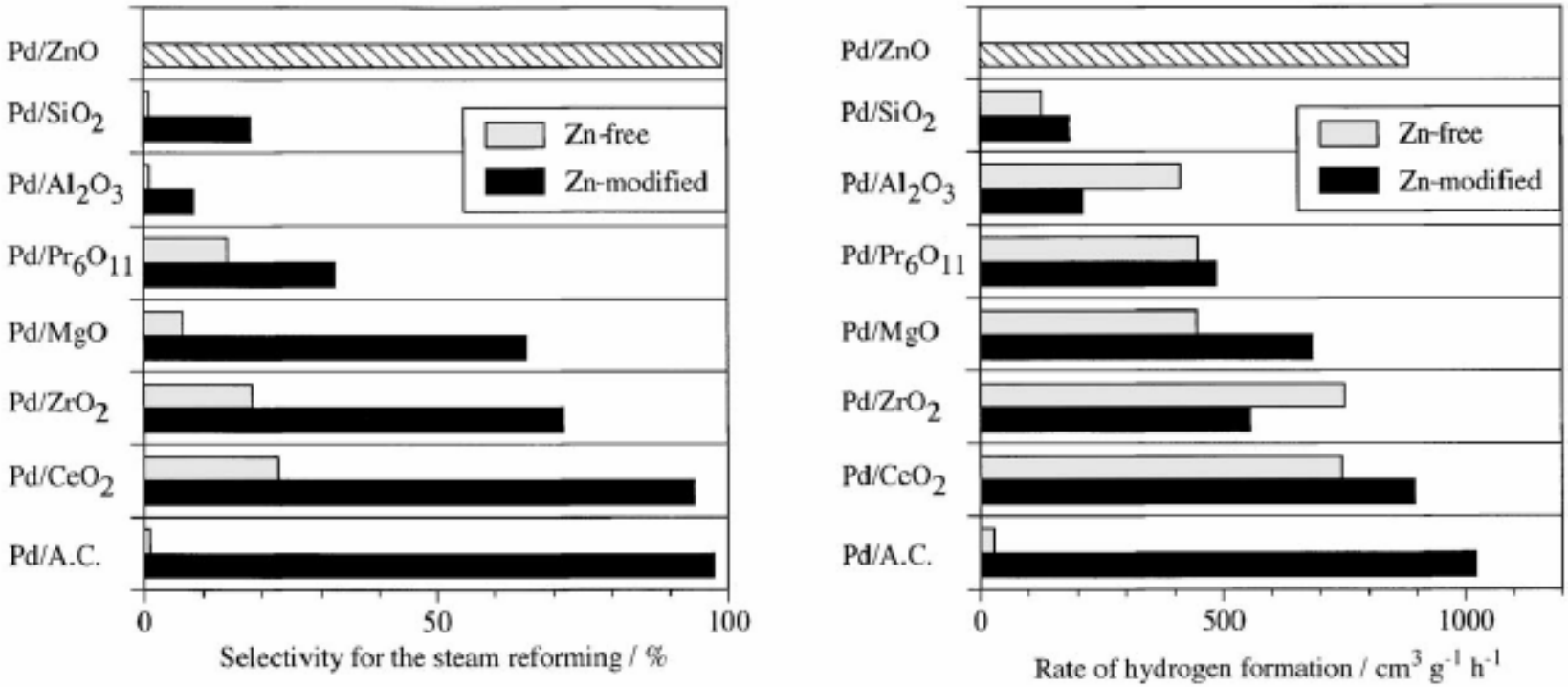

Pd Film Growth on ZnO(0001)

XPS

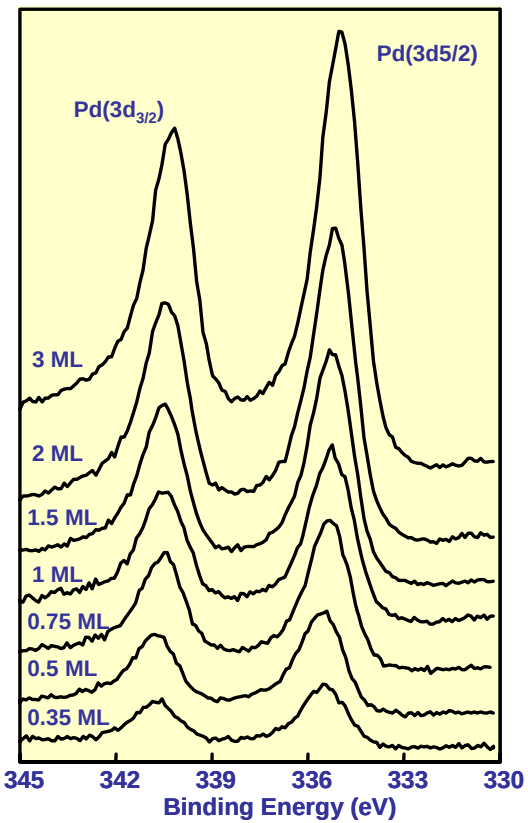

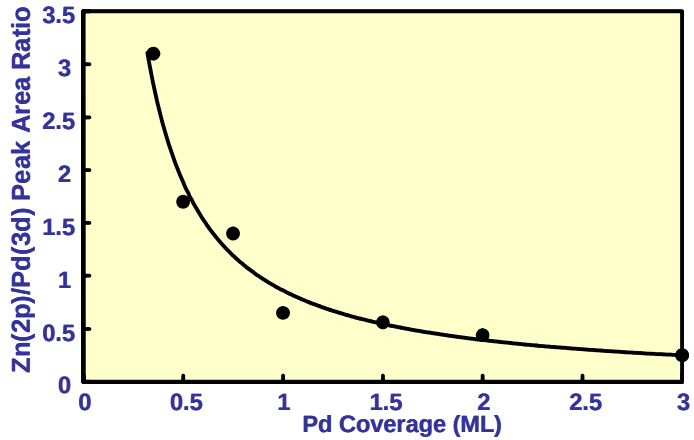

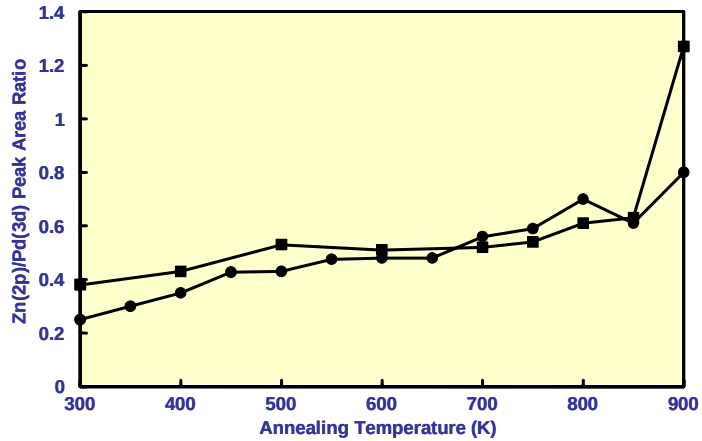

LEED

ZnO(0001)

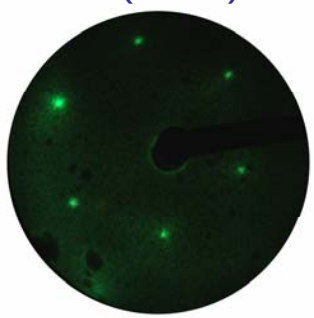

3 ML Pd/ZnO(0001)
300 K

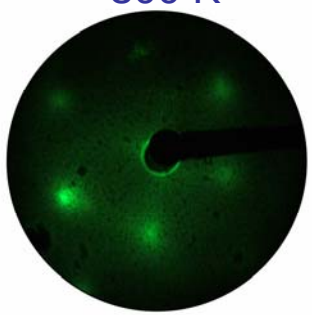

3 ML Pd/ZnO(0001)
850 K

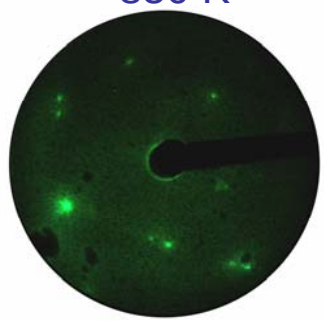

Growth of Pd Films on ZnO(0001) - Summary

XPS, LEED, HREELS indicate a 2D island growth mode

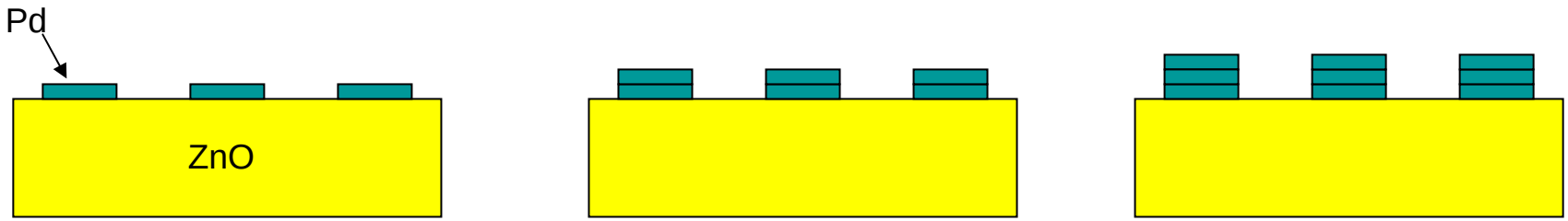

Critical island size ~0.5 ML

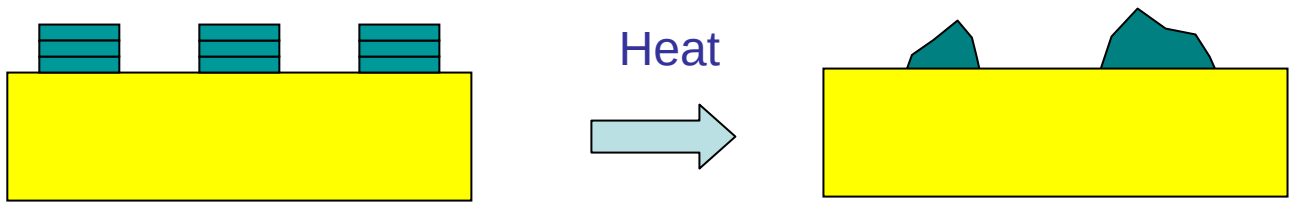

ZnO(0001), Pd/ZnO(0001) CH_3OH TPD

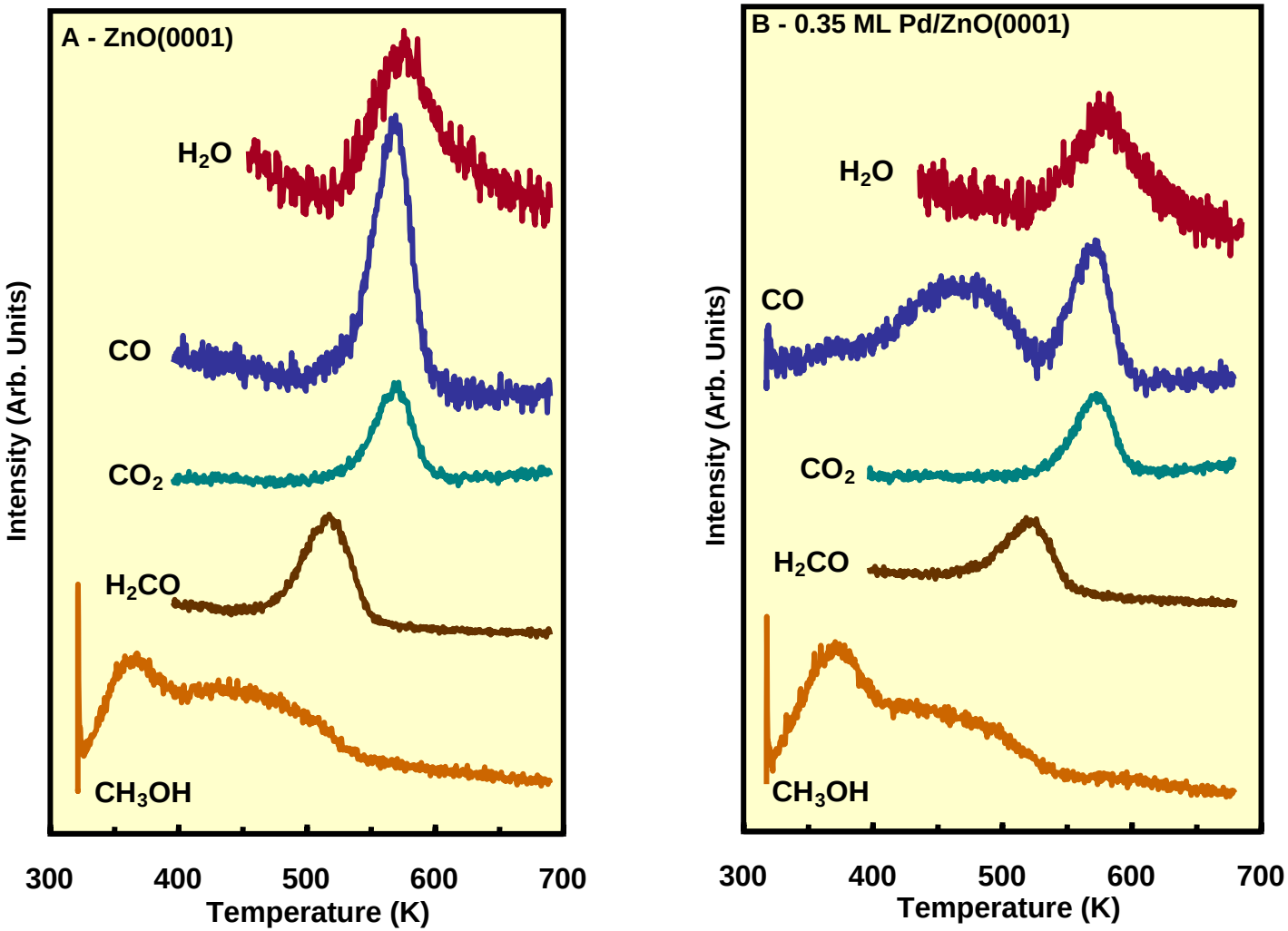

0.75 ML Pd/ZnO(0001) CH_3OH TPD

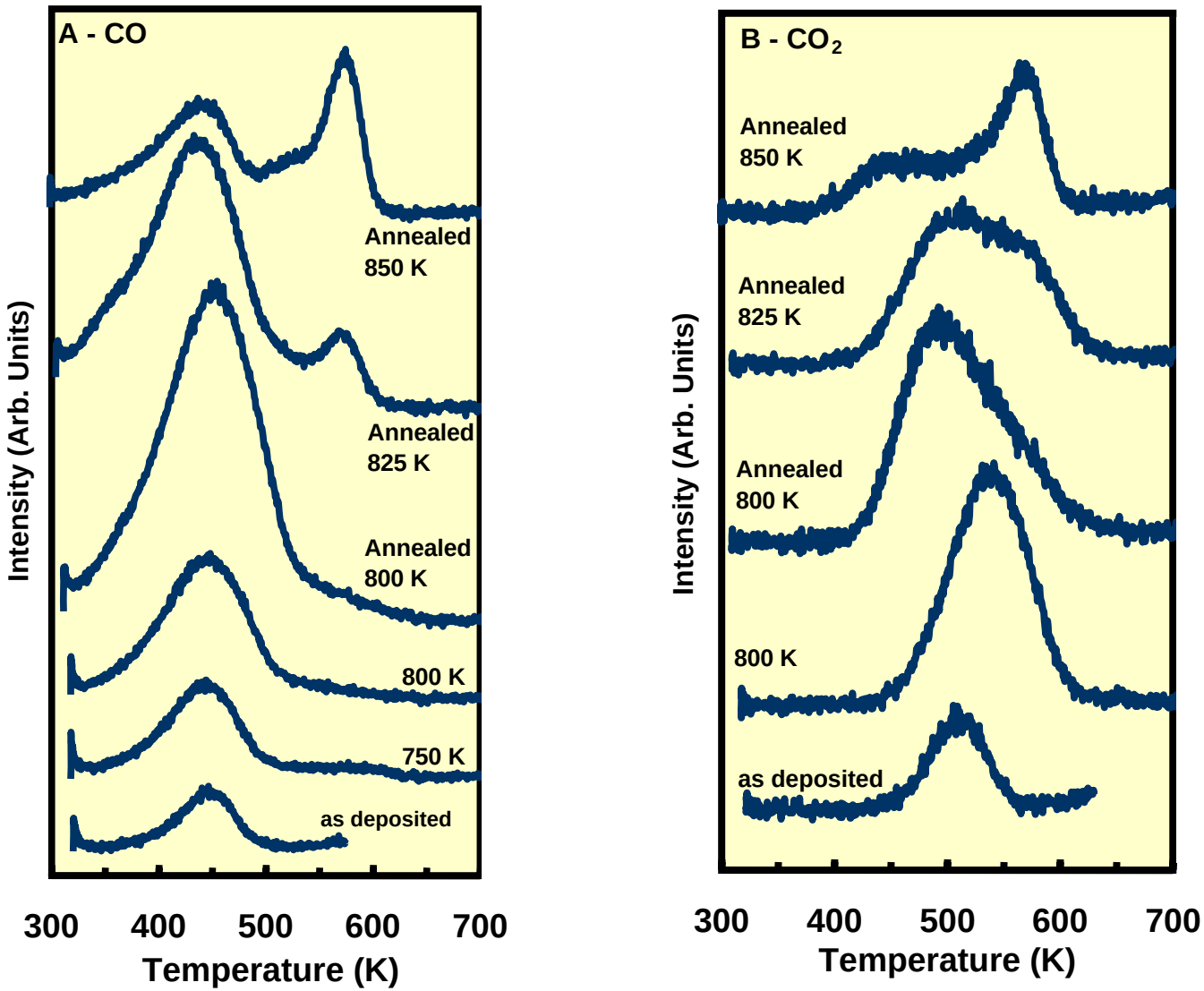

Pd/ZnO – high surface area catalyst

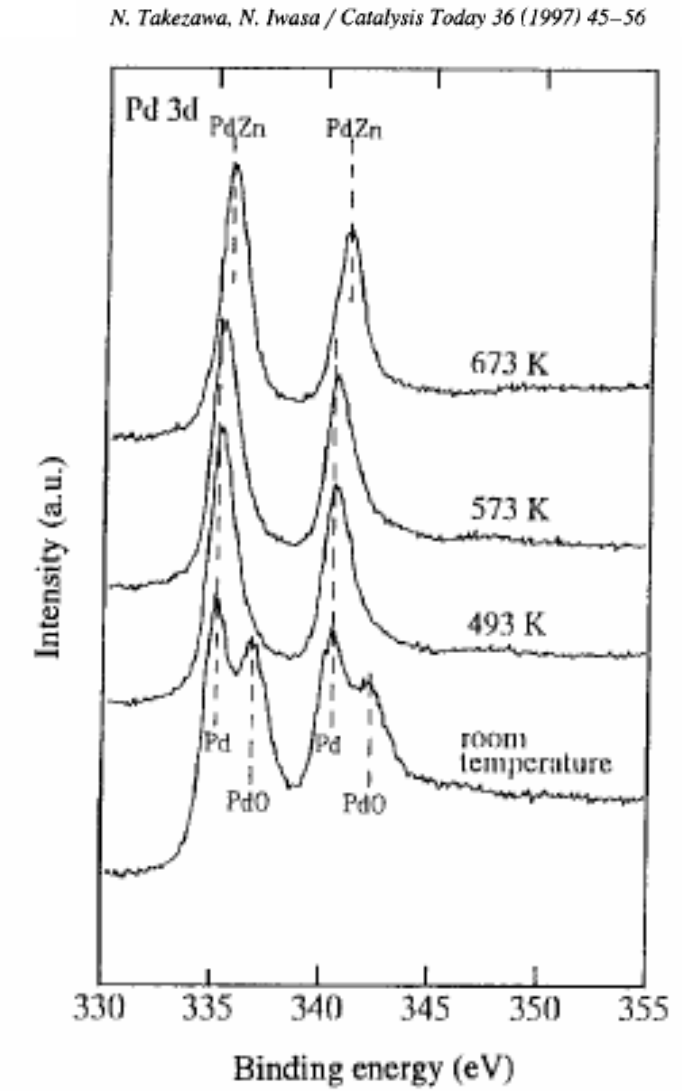

XPS spectra of 10 wt.% Pd/ZnO reduced in H_2 at various temperatures

Pd/ZnO(0001) – model catalyst

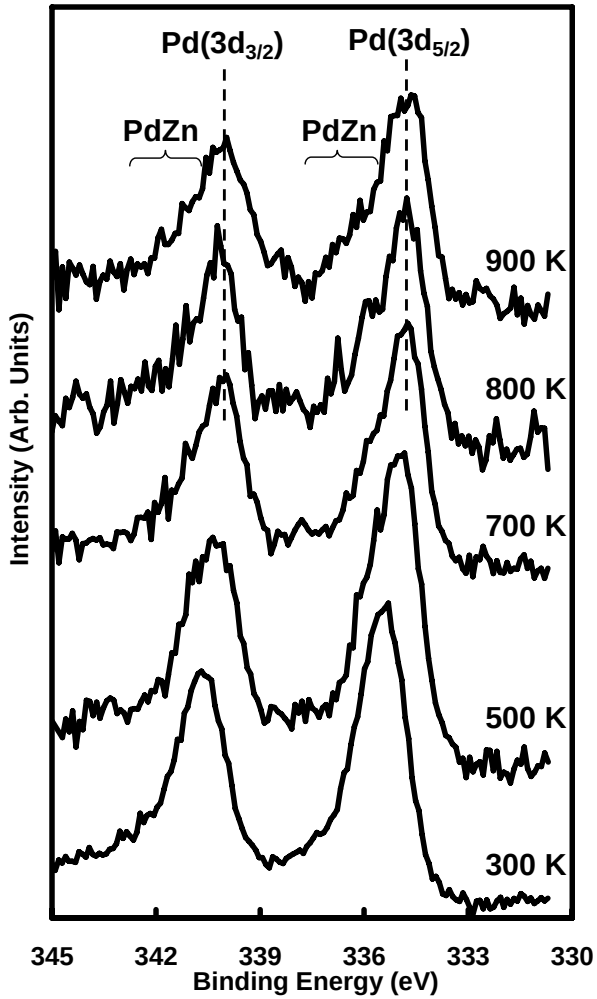

XPS spectra of 10 wt.% Pd/ZnO(0001) as a function of annealing temperature in UHV

Mechanism of the reaction of CH_3OH on Pd

250-300 K $CH_3O(ad) \rightarrow CH_xO(ad) + H(ad)$

$CH_xO(ad) \rightarrow CO(ad) + H(ad)$

$H(ad) + H(ad) \rightarrow H_2(g)$

450-500 K $CO(ad) \rightarrow CO(g)$

Proposed Mechanism for the production of CO_2 of CH_3OH on Pd/ZnO(0001)

300 K $CH_3OH + Pd \rightarrow CO\text{-}Pd + 2\ H_2(g)$

400-550 K $CO\text{-}Pd + ZnO \rightarrow CO_2(g) + PdZn$

In Pd/ZnO methanol steam reforming catalysts Zn may act as a redox site that provides oxygen for reaction with CO adsorbed on the metal to produce CO_2. These Zn sites could be located either at the Pd/ZnO interface or on the surface of the PdZn alloy.